5-2012

Parallel Adaptive Algorithms for Sampling Large Scale Networks

Kanimathi Duraisamy
University of Nebraska at Omaha

Parallel Adaptive Algorithms for Sampling Large Scale Networks

A Thesis Presented to the

Department of Computer Science and the Faculty of the Graduate College

University of Nebraska

In Partial Fulfillment of the Requirements for the Degree

Masters of Science

University of Nebraska at Omaha

By

Kanimathi Duraisamy

May, 2012

Supervisory Committee

Dr. Sanjukta Bhowmick, Chair
Dr. Hesham Ali
Dr. Parvathi Chundi
Dr. Dhundy Bastola

ProQuest LLC.
789 East Eisenhower Parkway
P.O. Box 1346
Ann Arbor, MI 48106 - 1346

Parallel Adaptive Algorithms for Sampling Large Scale Networks

Kanimathi Duraisamy, MS

University of Nebraska at Omaha, 2012

Advisor: Dr.Sanjukta Bhowmick

Abstract

The study of real-world systems, represented as networks, has important application in many disciplines including social sciences [1], bioinformatics [2] and software engineering [3]. These networks are extremely large, and analyzing them is very expensive. Our research work involves developing parallel graph sampling methods for efficient analysis of gene correlation networks. Our sampling algorithms maintain important structural and informational properties of large unstructured networks. We focus on preserving the relative importance, based on combinatorial metrics, rather than the exact measures. We use a special subgraph technique, based on finding triangles called maximal chordal subgraphs, which maintains the highly connected portions of the network while increasing the distance between less connected regions. Our results show that even with significant reduction of the network we can obtain reliable subgraphs which conserve most of the relevant combinatorial and functional properties. Additionally, sampling reveals new functional properties which were previously undiscovered in the original system.

Keywords: chordal graphs, parallel graph sampling, correlation networks, noise reduction, cluster overlap, edge enrichment score

Acknowledgements

It gives me great pleasure in acknowledging the support and help of my advisor Dr.Sanjukta Bhowmick who offered me invaluable assistance, encouragement, guidance and support throughout my thesis work. One simply could not wish for a better, friendlier and supportive mentor who could guide me through completion of this research. I am heartily thankful to Dr.Hesham Ali, without his knowledge and assistance this thesis would not have been successful. I am also grateful to Dr. Dhundy Bastola and Dr.Parvathi Chundi for all their constructive comments and valuable suggestions for my thesis work. I share the credit of my work with Ms. Kathryn Dempsey who helped me in obtaining the biological functional units.

My deepest gratitude goes to my family especially to my sister and brother-in-law, this research would have been simply impossible without their support and encouragement. I really want to thank all my family members for all their motivation and encouragement in all the areas of my life. I love to thank all my friends who where always there and supported me through this thesis.

Table of Contents

1. Introduction...1

1.1 Outline of Thesis...2

2. Background...4

2.1 Graph Terminology...4

2.2 Sampling..6

2.3 High Performance Computing...8

2.4 Gene Correlation Networks...8

3. Algorithm Description......... …..10

3.1 Data Structure..12

3.2 Chordal Graph Based Sampling...14

3.2.1 Parallel Algorithm with Communication...15

3.2.2 Parallel Algorithm without Communication.....................................18

3.3 Random Walk Based Sampling..19

4. Analysis of Results..21

4.1 Analysis of Combinatorial Properties...21

4.2 Analysis of Functional Properties...26

4.2.1 Analysis of Different Ordering..30

4.2.2 Analysis of Quality of Clusters...34

4.3 Analysis of Parallel Results..41

5. Conclusion..44

References...45

List of Figures

Figure 2.1: Example of Undirected Graph..4

Figure 2.2: Visual representation of graphs and their associated sampled subgraphs.......7

Figure 3.1: CSR format for a network..13

Figure 3.2: Original graph and it's maximal chordal subgraphs(sequential)..................14

Figure 3.3: Original graph and it's maximal chordal subgraphs(parallel).......................15

Figure 3.4: Visualization of networks for creatine mice dataset....................................16

Figure 3.5: Breakdown of execution time for obtaining QCS over different number of processors...17

Figure 3.6: Gene expression networks of the hypothalamus of a mouse brain and their respective Chordal graph representations...19

Figure 4.1: Degree distribution and average clustering coefficient of middle aged mice dataset...25

Figure 4.2: Degree distribution and average clustering coefficient of young mice dataset...25

Figure 4.3: Degree distribution and average clustering coefficient of creatine mice dataset...26

Figure 4.4: Degree distribution and average clustering coefficient of untreated mice dataset…………………………………………………………………26

Figure 4.5: Comparison of functional units of young mice dataset................................27

Figure 4.6: Comparison of functional units of middle aged mice dataset.......................28

Figure 4.7: Comparison of functional units of creatine mice dataset.............................29

Figure 4.8: Comparison of functional units of untreated mice dataset...........................30

Figure 4.9: Gene functionality of clusters for the young mice dataset with BFS ordering……………………………………………………………….....32

Figure 4.10: Gene functionality of clusters for the young mice dataset with RCM ordering...33

Figure 4.11: Example of how network sampling can positively or negatively affect the average edge enrichment score of a cluster by removing different sets of edge…..35

Figure 4.12: Example of how to identify the likely biologically meaningful cluster…...37

Figure 4.13: Node and edge overlap for original vs. sampled networks 38

Figure 4.14: Newly discovered nodes and edges for original vs. sampled networks......38

Figure 4.15: Sensitivity and specificity of filters for node and edge overlap..................39

Figure 4.16: Example of how filtering impacts a cluster..41

Figure 4.17: Scalability of sampling algorithms for a young and creatine mice network42

Figure 4.18: Parallel results for creatine natural order filter...43

List of Tables

Table 4.1: Comparison of combinatorial properties between the original network and chordal subgraphs………...23

Table 4.2: Comparison of combinatorial properties between the original network and random walk subgraphs...24

Chapter 1

Introduction

A network is a set of vertices and edges and has proved to be a useful abstraction for solving real world problems arising in systems of interacting entities. In a network model vertices represent the entities and the edges represent interactions, flow of information, degree of similarity or social relations between them. An advance in data collection, storage and retrieval has led to a proliferation of very large networks. However analyzing these networks, that is computing graph theoretic properties of the network and then relating them to the functionalities of underlying system, is a challenging task.

The underlying purpose of network analysis is to extract meaningful data from an application. However for large scale networks (Facebook has 8 million users) analysis process is both computation and memory intensive. Two popular techniques for reducing the use of resources are (i) using high performance computing to divide data over multiple processing units[4,5,6] (ii) sampling[7,8,9] that is extracting representative subgraph that exhibits similar characteristics to the original larger network.

A more insidious problem concerns noise in networks. Real-world networks are built using experimental (such as gene correlation networks) or subjective (census reports, epidemic distribution) techniques. The fluctuations and bias inherent in these methods would also be present in the form of small errors or noise within the network models. Let us take the famous example Facebook. The facebook algorithm suggests that you might know a person, because you have four mutual friends, which can be a good predictor of direct relationship. But sometimes Facebook can get it wrong because that person might be somebody whom you didn't met in your life. Such miscalculation occurs because not all connections in the Facebook are not of equal importance. Assuming equal importance to all edges is a form of noise. Once again selective sampling based on the analysis objective can reduce the noise in networks.

In this thesis, we developed scalable parallel network sampling algorithms that can filter out the noise, while preserving the important characteristics of the network. We compared two sampling techniques that are random walk and maximal chordal subgraph along with different permutations of the original network.

Our strategy is unique in that in contrast to other network filtering algorithms which only compare structural properties, whereas we compare both structural and functional properties. We validate our methods by using them to analyze gene correlation networks arising in murine models. Reduction of noise provides additional insight to the functional properties of the underlying application.

Our results show that chordal graph based sampling not only conserves clusters that are present within the original networks, but by reducing noise can also help uncover additional functional clusters that were previously not identifiable from the original network. We extend our research to investigate how different orderings affect the results of our sampling, and maintain the viability of resulting network structures. We show that our network sampling filter is a much better approach compared with other sampling filter like random walk.

1.1 Outline of Thesis:

This thesis is organized as follows. In Chapter 2, we provide brief overview and recent work in graph sampling. In Chapter 3, we describe our implemented newly developed parallel algorithm. In Chapter 4, we present our experimental results and analysis which include comparing both combinatorial and functional properties of original network and subnetworks. In Chapter 5, we discuss our concluding remarks and present potential ideas for further research.

Chapter 2

Background

Graphs are among the most ubiquitous models of both natural and human-made structures. They can be used to model many types of relations and process dynamics in physical, biological [13] and social systems. Many problems of practical interest can be represented by graphs. Graph is a collection of vertices and a collection of edges that connect pairs of vertices. Graphs are represented graphically by drawing a dot or circle for every vertex, and drawing an arc between two vertices if they are connected by an edge. If the graph is directed, the direction is indicated by drawing an arrow.

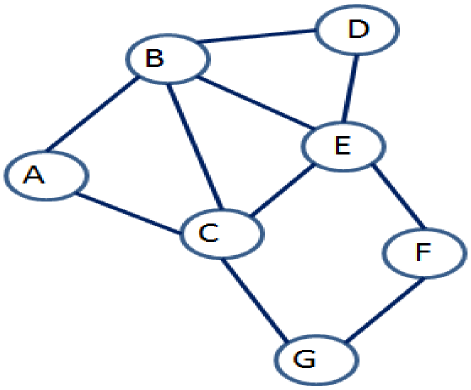

Figure 2.1: Example of Undirected Graph

2.1 Graph Terminologies:

We introduce some graph terminology that will be useful in the subsequent explanation of the algorithms (based on the definitions provided in [10]).

Vertices and Edges: A graph G= (V, E) is defined as a set of vertices V and set of edges E. An edge e € E is associated with two vertices u, v which are called its endpoints. A vertex u is said to be a neighbor of vertex v, if they are joined by an edge. In Figure 2.1, there are total 7 vertices and 10 edges in the graph.

Cycle: A Path is an alternating sequence of vertices and edges, where subsequent vertices are connected by an edge. A Cycle is a path where the initial and final vertices are identical. In Figure 2.1, vertices (A, B, E, C, A) forms cycle.

Clique: A Clique is a set of vertices that are all connected to each other. In Figure 2.1, vertices (A, B, C) forms clique because everyone in the group is connected to each other. Some other cliques are (B, E, C) and (B, E, D).

Degree: Degree of a vertex in a graph is the number of edges the vertex has with the other vertices. The Degree of vertex v is denoted as deg(v). Vertices with high degrees are called hubs. In Figure 2.1, Degree of vertices are, deg(A) = 2 , deg(B) = 4, deg(C) = 4, deg(D) = 2, deg(E) = 4, deg(F) = 2 and deg(G) = 2.

Degree Distribution: Degree Distribution is the probability distribution of degrees of the vertices over the network. Degree distribution is (d_1, d_2… d_{n-1}), where d_k is the number of vertices with degree k. Degree Distribution for graph in Figure 2.1 is (0, 4, 0, 3, 0). Most scale free system like social and biological networks observe a power law based distribution [29] that is there are many vertices with low degree and the number of vertices exponentially go down as the degree increases.

Clustering Coefficient: Clustering Coefficient is a measure of degree to which nodes in a graph tend to cluster together. It is calculated as the ratio of the edges between the neighbors of a vertex to the total possible connection between them. The higher the clustering coefficient it is more likely that a vertex is part of a dense module with closely interconnected dependencies. In Figure 2.1, Clustering Coefficients values of vertex A = 1, vertex B = 0.5, vertex C = 0.3, vertex D = 1.0, vertex E = 0.3, vertex F = 0, vertex G = 0.

Core Number Distribution: Core Number of a vertex is defined as the largest integer c such that the vertex exists in a graph where all degrees are greater than equal to c. The higher the value, the better the clustering property should be maintained. In Figure 2.1, Core Number of all vertices is 2.

Chordal Graph: A Chordal Graph is a graph where the length of a cycle is be no more than three.

2.2 Sampling:

Graph Sampling involves extracting a representative subgraph that exhibits similar characteristics to the original, larger network. Usually sampled graphs reliably estimate the dynamicity of the network, that is a small change in the network would represent a small change in the sampled graphs and an important change in the larger network would considerable modify the sampled graph. They focus on preserving the relative values rather than the exact ones. For example, preserving the degree distribution even if the values of the degrees and might have changed.

In Figure 2.2, A shows a network with 99 vertices and 253 edges, (highest degree 11 and lowest degree 1). We perform two modifications on the graph,–the first by removing a vertex of degree 1(Figure B) and the second by removing a vertex of degree 10(Figure C). On visual inspection, it is very difficult to spot the difference between the graphs in the top level. However, in their sampled graphs we see that A’ and B' look similar indicating the small change in original graph. Whereas A' and C' look different representing a more significant change.

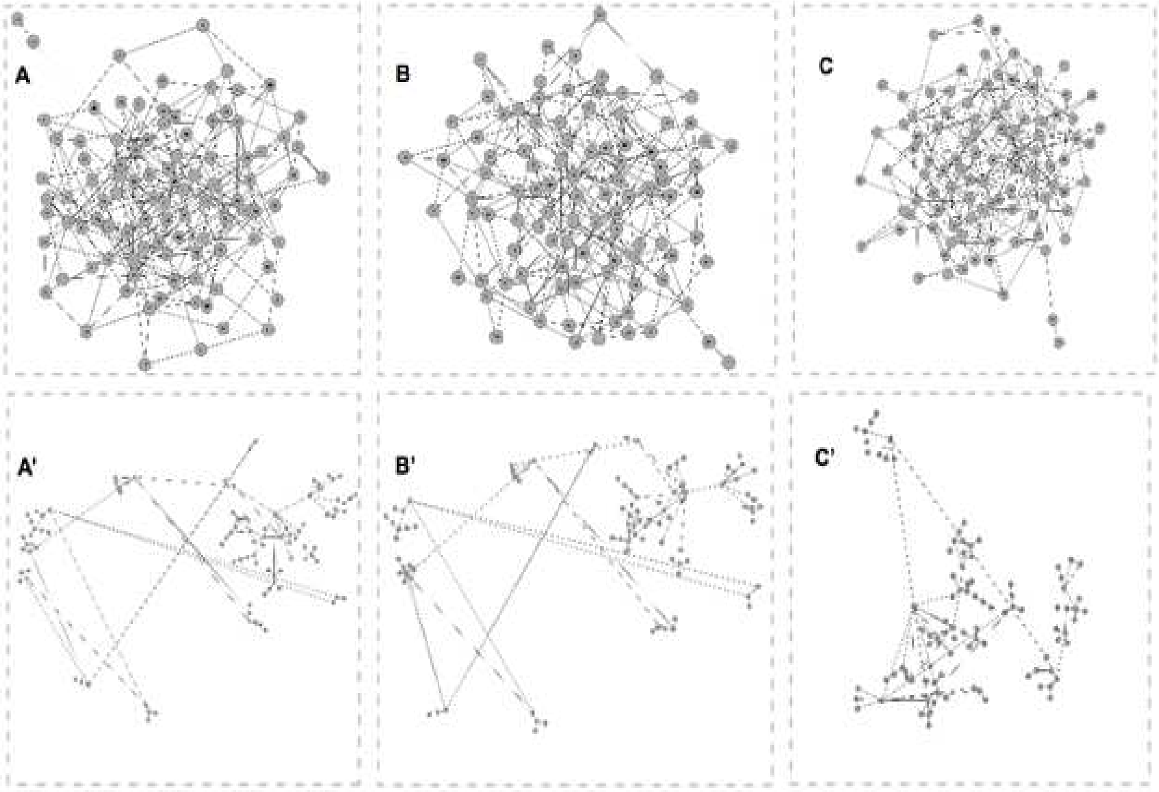

Figure 2.2: Visual representation of graphs and their associated sampled sub graphs.

Graph sampling is effective in reducing data and computational costs while preserving the accuracy of analysis results. Previous work [11] focused on sampling the networks for better visualization. Degree distribution and component size distribution are the two important visual feature of a network they are interested. Whereas Gilbert[12] aimed at graph compression for visualization that preserves the semantics of the original graph.

Most sampling methods for large scale-free networks are based on random sampling, such as random node selection or random walks on the network. Leskovic [7] stated that random walks and forest fire are good at extracting samples from large networks. They are interested in finding a general sampling method that would match a full set of graph properties. A recent work [14] analyze the result of various sampling algorithms using three different measures namely Degree, Clustering and Reach. Most of the previous work concerned with constructing samples that match structural properties of the original network.

A parallel version of random walks is based on starting multiple walks simultaneously on different processors [15]. Parallel algorithms for obtaining spanning trees such as breadth first trees, connected components and minimum spanning trees on large-scale networks are also being investigated [4,5,6].However the spanning tree methods focus more on graph traversal than sampling important regions.

Filtering noise for large networks is still a largely unaddressed problem Some recent work has focused [16,17] on using machine learning techniques to detect noise in biological networks and uses supervised learning to predict noise based on prior information.

Our algorithm effectively select good representative samples of a large graph that can filter out the noise, while preserving important characteristics of the network so that sampled graphs can be used for more complicated experiments.

2.3 High Performance Computing:

With the increase in data and problem sizes, high performance computing has become an essential tool for efficient implementation of large scale applications. In the sequential programming, processes are run one after another in a succession fashion and it's expensive. In high performance computing, we have multiple processes execute at the same time and so we can complete time consuming operation in less time.

2.4 Gene Correlation Networks:

A correlation network is represented as a graph, where vertices represent genes and edges represent the correlation between the expression levels of two genes. Gene correlation networks are created based on the correlation between expression levels of different genes as obtained from microarray data analysis. Different measurements of correlation have been used to build these networks, such as the partial correlation coefficient [19], the Spearman correlation coefficient [20] and more commonly, the Pearson correlation coefficient [21].There are many methods for thresholding the correlation network. The most straightforward involves removing edges with a low correlation. In a larger network created using the Pearson correlation coefficient, we use a threshold of ±0.70 to ±1.00 based on the fact that the coefficient of determination for these correlations will be at least 0.49.

The degree distribution of correlation networks follows a power-law distribution [22] that indicates a scale-free network structure. Adherence to this distribution indicates that there are many nodes in the network that are poorly connected and a few nodes that are very well connected; these nodes are known as "hubs”. A primary analytical operation of correlation networks is identifying high density clusters of genes, represented by tightly connected vertices in the network. Analyzing these networks is a computationally expensive which creates the need for efficient sampling mechanisms. Furthermore, correlation networks can have noise or unnecessary edges, which can adversely impact the accuracy of the results.

Chapter 3

Algorithm Description

Graph sampling should represent the relevant features of the larger network especially structural and informational properties that helps to improve the interpretation of large networks**.** Moreover, sampling is effective in reducing computational and data costs and also the sampled subgraph occupies less memory than original network. The objective of our sampling algorithm is to maintain the highly connected subgraphs like cliques from the original network while removing some of the associated noise. We assume that the effect of noise is more likely to be prevalent in structures formed by loosely connected vertices. Spanning subgraphs which includes all the vertices and some edges of the graph such as Minimum Spanning Tree, Steiner Tree, Planar Tree, Random Walk and Chordal Subgraphs possess many of the these properties to sample a graph perfectly.

For a given graph/network, Minimum/Maximum Spanning Tree (MST) is a subset of all edges that connects all nodes at minimum/maximum total weight without cycles. The heaviest edge in any cycle cannot be in the minimal spanning tree. Moreover, the lightest edge in any cut must be in the minimal spanning forest. so we cannot guarantee that all the important functional properties would be retained in sampled graph. In addition, all the cycles will be deleted in spanning tree which means it can't keep densely connected regions.

Steiner Tree problem is superficially similar to the Minimum Spanning Tree problem: given a set V of points (vertices), interconnect them by a network (graph) of shortest length, where the length is the sum of the lengths of all edges. The difference between the Steiner Tree problem and the Minimum Spanning Tree problem is that, in the Steiner Tree problem, extra intermediate vertices and edges may be added to the graph in order to reduce the length of the spanning tree. Adding more information to the Steiner Tree distort the values present already present in network.

Planar Graph is a graph which can be drawn in the plane (e.g. on a piece of paper) without any of the edges crossing over, that is, meeting at points other than the vertices. Several important graph theoretic concepts were discovered by looking at planar graphs. The notion of vertex coloring of graphs came from the four color conjecture about planar graphs. Similarly, Hamiltonian paths and cycles were studied for planar graphs. But if the original network has clique of 5 or a complete bipartite graph with 3 nodes on each side, then subgraph will not be retained in sampled graphs. We found it is difficult to retain almost all densely connected regions in planar graph.

In the recent years, many researchers have focused on random walk in graph sampling area [7]. A Random Walk selects the next node at random from among the neighbors of the current node. Random Walk has a good chance of finding densely connected regions in large network. This motivated us to do some background research on this area and write parallel code to extract a subgraph from the larger network. As expected, sampled subgraphs find clusters from larger network. We went a step ahead and analyze the quality of those clusters. Unfortunately, the sampled graph using Random Walk did not retain the important biological properties.

Chordal Subgraph is a spanning subgraph of the network where there are no cycles of length larger than three. This interesting family of graphs is not only good for sampling, but Chordal Subgraphs preserve many topological features such as the number of triangles, the number of cliques, and the lower bound on the number of colors. Choices of edges to be retained in Chordal graphs are based on information content which indicates that sampling based on Chordal graphs will retain important informational properties of the network. Due to these properties of the Chordal graphs, they can be used to construct efficient linear time algorithms for non-polynomial problems such as minimum coloring and maximum cliques. It provides the approximation of the larger graph to obtain near exact results with low computational cost and also the complexity of finding Chordal Subgraph is O(|E|*max_deg)[18]. Retrieving Maximum Chordal Subgraph from the given network is NP hard problem so we decided to go with Maximal Chordal Subgraph based on the algorithm provided by Dearing et. al.[18] to maintain the densely connected regions in the sampled subgraph.

3. 1 Data Structure:

Compressed row storage method [33] is a popular format for representing elements of sparse matrices. The storing the non-zero elements of a sparse matrix into a linear array is done by walking down each column or across each row in order, and writing the non-zero elements to a linear array in the order they appear in the walk.

Graphs can be represented as an adjacency matrix where rows and columns are labeled by graph vertices and value of adjacency matrix (V_i, V_j) is 1 if there is an edge between vertex V_i and vertex V_j otherwise 0 . In this method all the information is stored into three vectors as described below.

(a)**Values**: stores the non-zero values of a sparse matrix by walking down each column and writing a non-zero values

(b) **Columns**: Value of Columns[i] is the number of the column of adjacency matrix that contains the Values[i] element.

(c) **Row Index**: Value of Row Index[i] gives the index of the element of the Values array of the first non-zero element in a row ‘i’ of adjacency matrix.

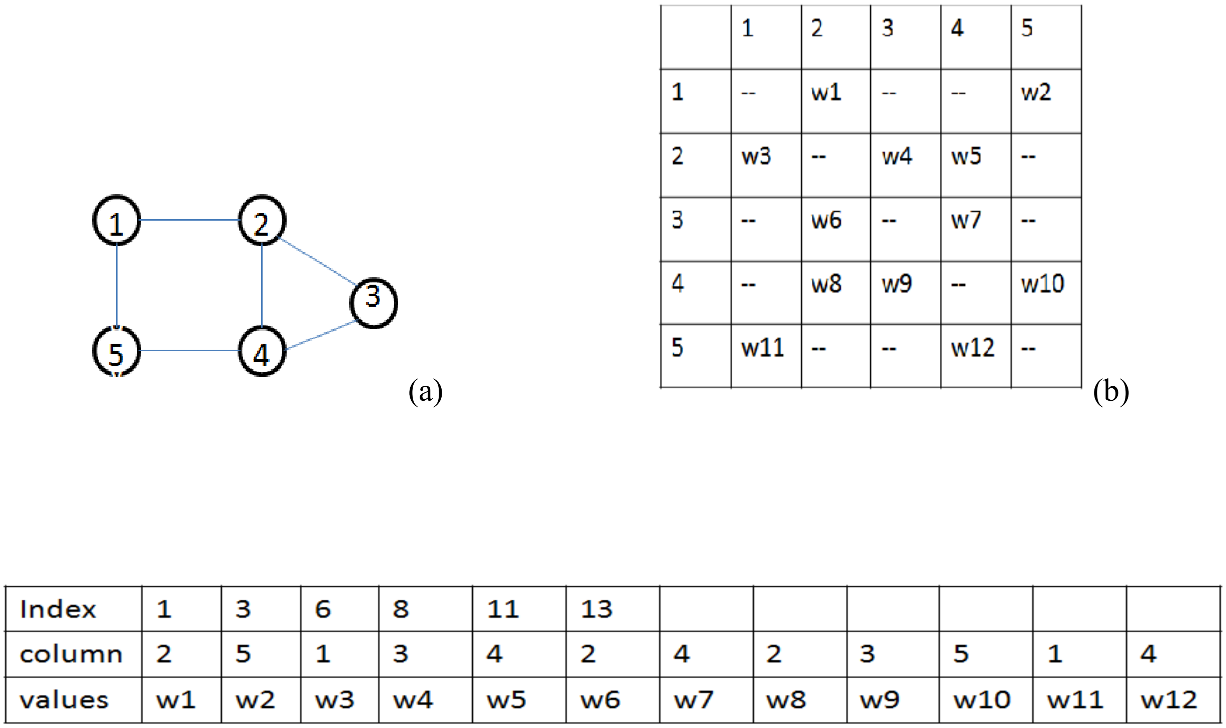

(a)

	1	2	3	4	5
1	--	w1	--	--	w2
2	w3	--	w4	w5	--
3	--	w6	--	w7	--
4	--	w8	w9	--	w10
5	w11	--	--	w12	--

(b)

Index	1	3	6	8	11	13					
column	2	5	1	3	4	2	4	2	3	5	1	4
values	w1	w2	w3	w4	w5	w6	w7	w8	w9	w10	w11	w12

(c)

Figure 3.1 CSR format for a network a) The original network of 5 vertices b) The sparse adjacency matrix corresponding to the network. c) The CSR format for the sparse matrix

3.2 Chordal Graph Based Sampling:

Our sampling technique for obtaining the maximal chordal subgraph is provided by Dearing et. al. [18]. This method is based on growing the graph from a starting vertex and adding edges as long as they maintain the chordal characteristics. Initially the chordal subgraph consists of the starting vertex and its associated edges. In the subsequent steps, the vertex with the maximum number of visited neighbors is selected. An edge from the current selected vertex a, (a,b) is added to the chordal subgraph if the number of visited neighbors of b is a subset of the number of visited neighbors of a. The complexity of this algorithm is O(Ed) where E is the number of edges in the graph and d is the maximum degree.

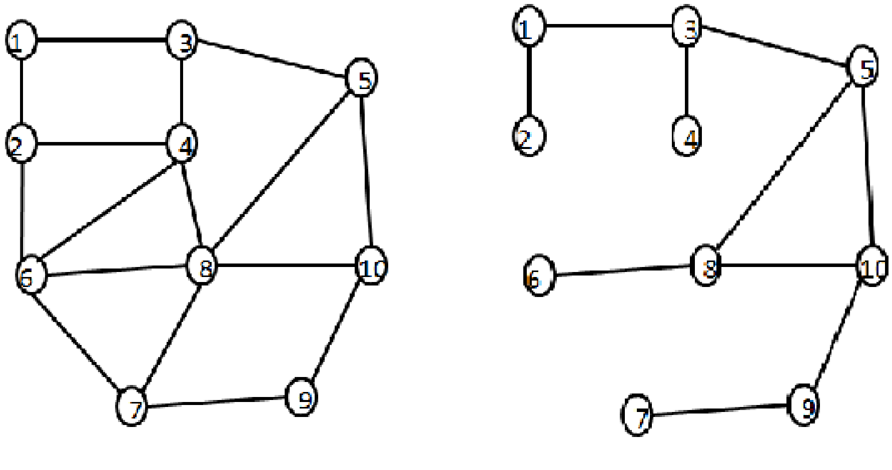

Figure 3.2: Original Graph (Left) and it maximal chordal subgraph(Right)

The sequential algorithm for finding MCS and indeed most of the sampling methods assume that the original network is connected. However, many real-world networks, such as our test suite of gene correlation networks have disconnected components. Based on our initial tests, we discovered that a completely chordal subgraph is a very strict restriction, and can disintegrate some clusters, that are almost, but not exact, cliques. To counteract this effect we modified the algorithm to extract quasi-chordal subgraphs, which can include few cycles of length greater than three. We believe that more loosely coupled structures are potentially eliminated in quasi chordal subgraph by including only border edges that are part of at least one triangle. In order to accommodate large networks, we have developed and implemented a parallel algorithm for extracting the maximal chordal subgraphs from the network. These subgraph preserves most of the cliques and highly connected regions of the network which increases the path lengths between loosely connected regions. We validate our algorithms by applying them to analyze gene correlation networks.

3.2.1 Parallel Algorithm with Communication:

Our parallel implementation on a distributed memory system was follows: We divided the network across P processors, and identify the local maximal chordal subgraph

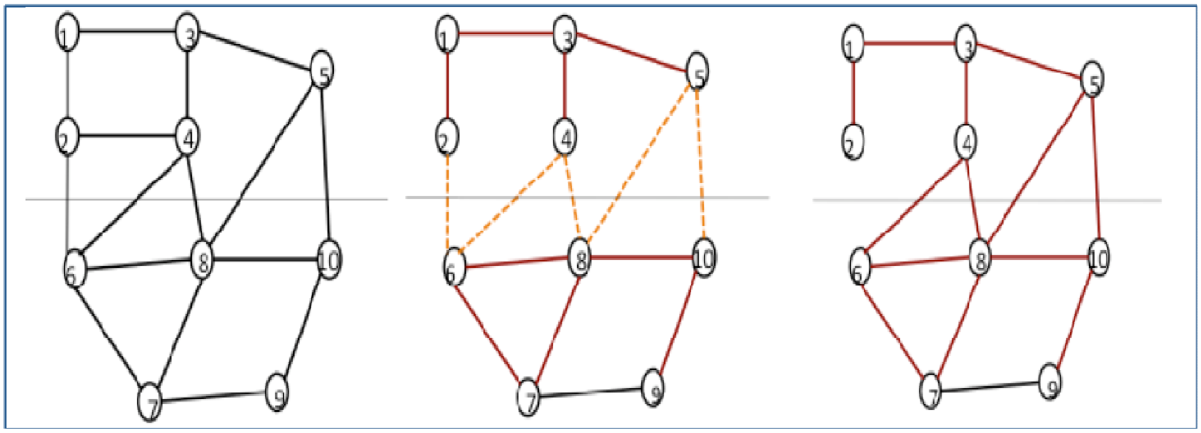

Figure 3.3: Original graph and their associated maximal chordal subgraphs

formed only of the edges whose endpoints lie completely within a processor. Next, we identify the border edges whose endpoints lie across the partitions. For each pair of processors we identified a receiver where the synchronization would take place. We assign the processors as sender and receiver in such a way that computation load is balanced across all processors. We sent the border edges to designated receiver processors. The edges that lie across processors is included only if two border edges with a common vertex combined with a previously marked chordal edge to form a triangle. This implementation generated quasi-chordal subgraphs (QCS), since the inclusion of border edges can sometimes increase the length of cycles by more than three.

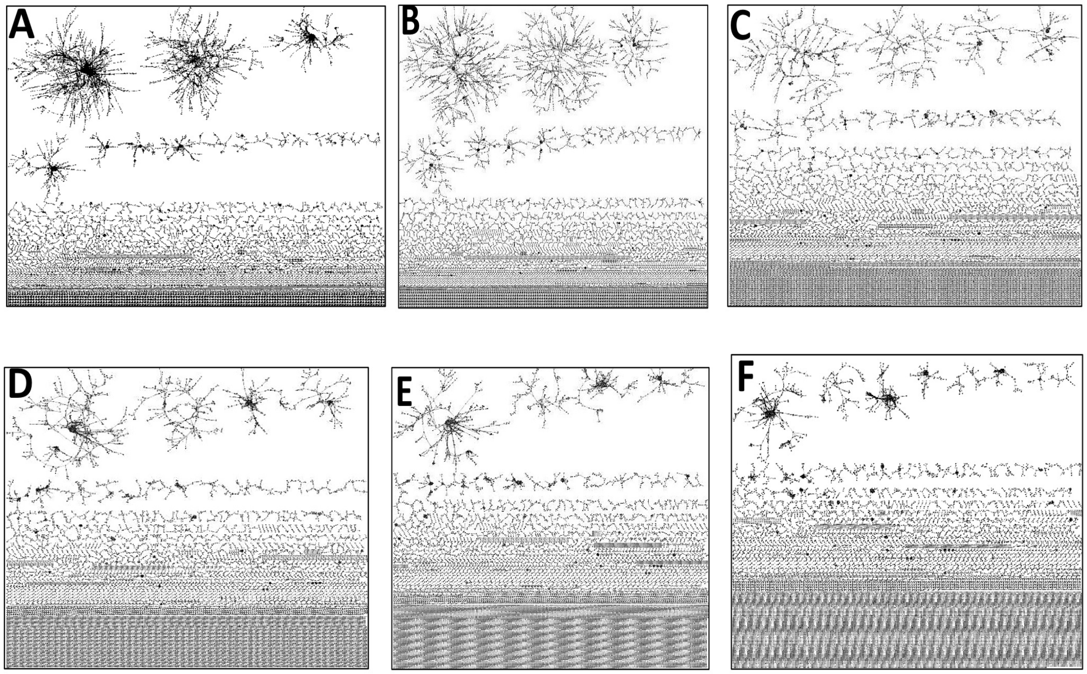

Figure 3.4: Visualization of networks from the creatine treated mice. A: Original Network. B: QCS with 1 Partition: QCS with 2 Partitions. D: Left Figure: QCS with 4 Partitions. E: QCS with 8 Partitions. F: QCS with 16 Partitions.

Figure 3.4 shows the QCS generated from one of our sample networks. The scalability of our parallel algorithm can be computed as follows; Let the number of edges in the network be E, the maximum degree of the network be d and the number of processors involved be p. The complexity of the sequential algorithm is given by $T_{seq}(E) = O(Ed)$. The parallel overhead $T_{over}(E,p)$ consists of communicating the border nodes from each processor, denoted by b, and subsequently checking, for each pair of border nodes, if they form a triangle with a chordal edge. Assuming equal distribution of border nodes, the total communication volume is O(bp) and the computation volume over all processors is $O(b^2p)$. Therefore, $T_{over}(E,p) = O(b^2p)$. In order maintain isoefficiency, $T_{seq}(E) >= T_{over}(E,p)$, which implies $E >= Cb^2p/d$, where C is a constant. The memory required by to store the network is approximately O(E). Therefore, the scalability function for this algorithm can be computed as $(Cb^2p)/(dp) = O(b^2/d)$. Thus, the parallel overhead increases with the number of border edges.

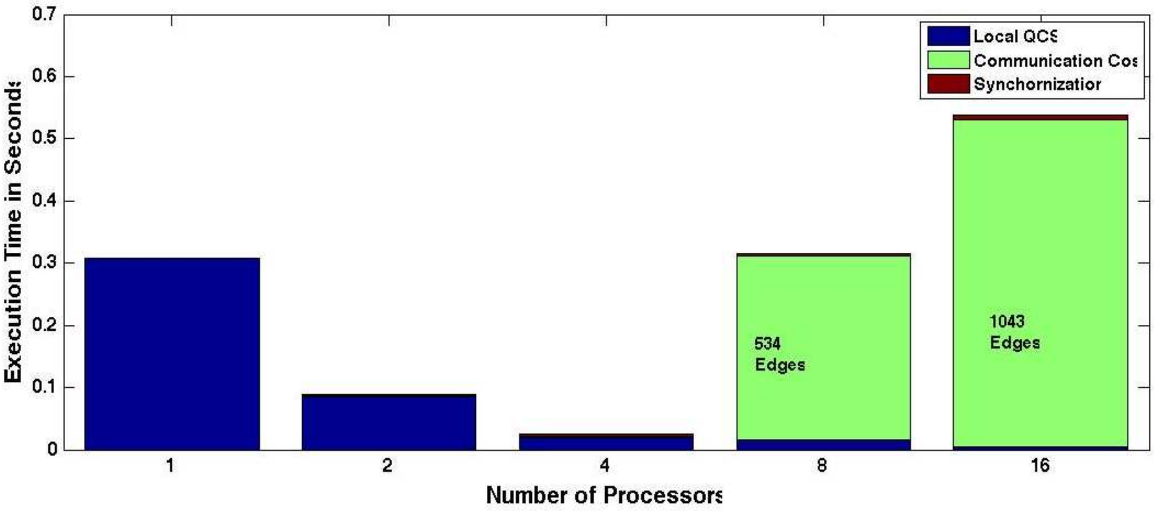

Figure 3.5: Breakdown of execution time for obtaining QCS over different number of processors. As the number of processors increase, the communication overhead for the border edges outweighs the gains due to parallelization.

A limitation of this implementation is that the algorithm does not scale well. If the network is too small and number of processors is large, then b increases. Again, if the network is too big and there are fewer of processors, then too b increases significantly.

Additionally, depending on the distribution some processors might have more border edges to analyze as compared to other processors.

Figure 3.5 shows the breakdown of the execution times of the different sections of the algorithm over 1,2,4,8 and 16 processors. As can be seen from the figure the time to compute the local QCS (blue blocks) gradually decreases over the number of processors. However, the communication costs (border edges) keep increasing with the number of processors, which finally leads to significant increase in the execution time.

3.2.2 Parallel Algorithm without Communication

Primary goal is to reduce the communication costs and maintain a better balance of the workload.

In this version, graph is partitioned as before, and then chordal edges and border edges are marked. Instead of sending the border edges to the receiver, we simply compare them with the local chordal edges. Pair of border edges is included in the subgraph if they form a triangle with already marked chordal edge. In Figure 1, edges (2, 6) and (4, 6) will not be included in the top partition because (2, 4) is not a chordal edge. However in the bottom partition (4, 6) and (4, 8) are included since (6, 8) is a chordal edges and so are (5, 8) and (5, 10). This implementation requires no communication and provides a more equitable distribution of the workload. It is therefore more scalable than our earlier algorithm.

Because multiple processors can work on the same border edge, it is likely that some of the border edges will be represented twice in the final filtered subgraph. During analysis, which is done sequentially, we have to remove these duplications. In the worst case there can be as many as b duplications, where b is the number of border edges.

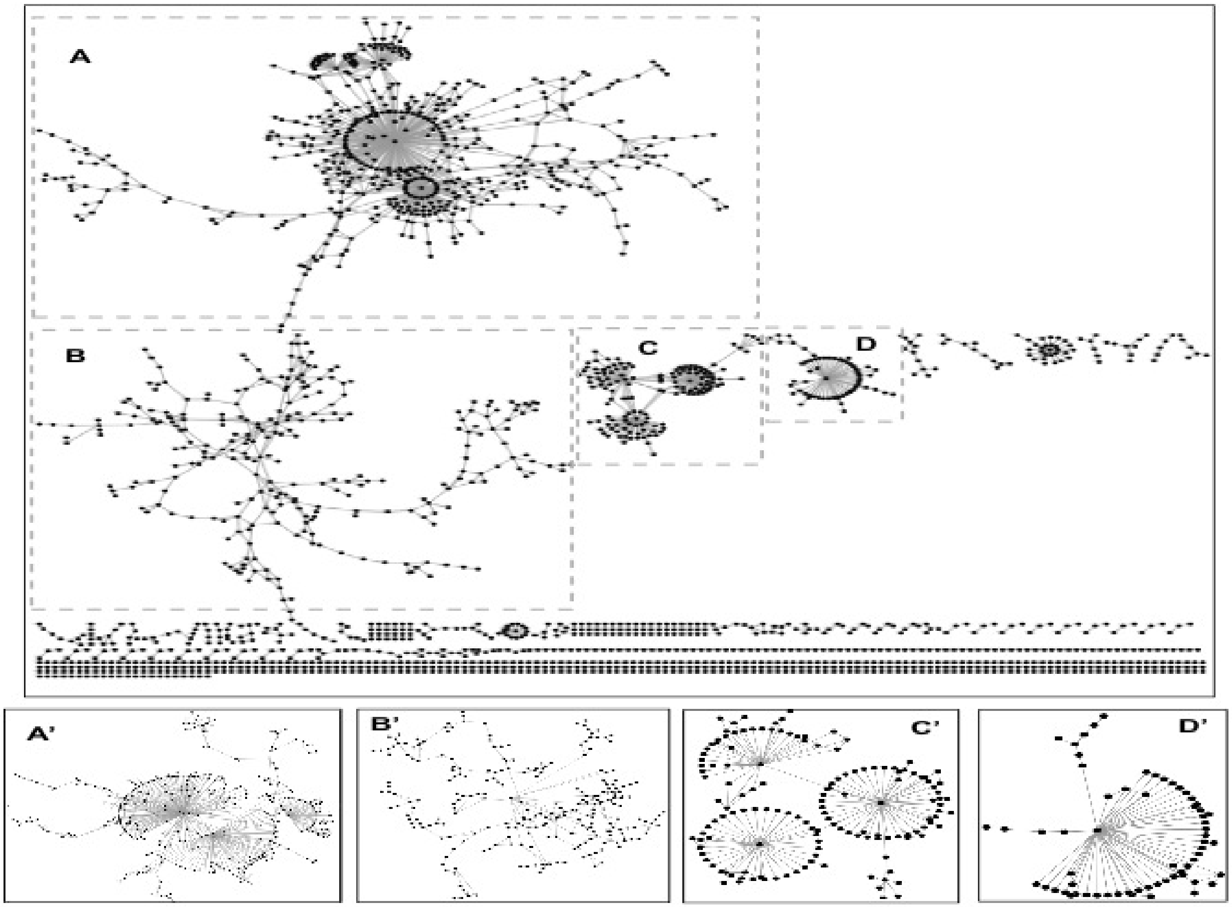

Figure 3.6: Gene expression network of the hypothalamus of a mouse brain with larger components highlighted in broken line boxes (A-D) and the respective chordal graph representations shown below (A'-D'). The chordal graphs preserve the structure but have significantly lower number of edges.

Our primary contribution is in developing a parallel sampling technique for large-scale networks that not only extracts important combinatorial properties, but also eliminates some of the inherent noise in the networks. Reduction of noise provides additional insight to the functional properties of the underlying application. Figure 3.6

demonstrates how QCS based sampling can effectively select good representative samples of a large graph.

3.3 Random Walk Based Sampling:

In order to compare the effectiveness of our method, we also implemented a parallel random filtering method. The random walk was also designed as a variation on graph traversal. At each vertex of degree *d,* one of its associated edges was selected with probability *1/d*. The graph traversal was completely random in that we did not maintain a list of which edges or vertices have been visited, and a vertex could be visited multiple times. The rationale for random walk is that tightly connected groups of vertices will have a higher chance of being repeatedly selected and therefore cliques and other highly connected regions would be preserved in the filtered graph. The traversal process is continued iteratively until the number of times edges are selected is half the total number of edges in the network.

The parallel random walk algorithm also divides the network across processors and as in the case of the chordal graph based sampling, each processor finds its local random walk based subgraph. Each border edge is associated with a binary random value, and based on the value the edge is either included in the subgraph (e.g. for value 1) or not (e.g. for value 0). However, the addition of the border edges is much simpler. This algorithm is of course perfectly scalable as again no communication is required for the border edges. The random walk filter would also require less execution time than the chordal graph filter, because the choice of the next edge is much simpler.

Chapter 4

Analysis of Results

The datasets GSE5140 and GSE5078 for our experiments were obtained from NCBIs Gene Expression Omnibus (GEO) website (http://www.ncbi.nlm.nih.gov/geo/) and divided based on age/treatment [23, 24]. GSE5078 was divided into young mice (YNG) and middle-aged (MID) mice data (2 months and 15 months respectively). GSE5140 was divided into untreated middle-aged mice (UNT) and creatine-supplemented middle-aged mice (CRE) datasets [24]. Both datasets were designed to identify age-related changes in brain tissue from mouse models at different ages/states. These Networks were created by pairwise computation of the Pearson correlation coefficient for each possible pairing of the genes and thresholding was applied to eliminate low correlation edges.

We obtained quasi-chordal subgraphs for these four networks, by the process described in Section 3 on 1,2,4,8 and 16 processors on a distributed memory system using MPI. The codes were executed on the University of Nebraska at Omaha's Blackforest linux computing cluster, consisting of subclusters of Intel Pentium D, Dual-core Opteron and 2 Quad-core AMD Opteron processors.

Our empirical results fall into three categories. The first involves analysis of comparing the combinatorial properties of the networks and the subgraphs. The second deals with functional units in the correlation networks and also detailed analysis of the clusters obtained. The third deals with the parallel sampling algorithm their scalability and effect on analysis of data.

4.1 Analysis of Combinatorial Properties:

Table 1 compares the combinatorial properties including reduction in edges, degree distribution , clustering coefficients, number of vertices with high degrees (hubs) and high core numbers using MatlabBGL library [25].The numbers in the parenthesis denote the reduction percentages. The best values of edge reduction, hub and core number retention are marked in bold.

As expected, the subgraphs have lower number of edges, the higher the number of processors, the more the reduction. The percentage reduction is computed by 1-(Edges in Subgraph/Edges in Original Network). The higher the number, the more the reduction.

Degree distribution is computed as number of vertices with degree d. Degree distributions in the correlation networks follows the power law. We also compare the average clustering coefficients per degree between the networks. The value of subgraphs should be close to the original network. We compare how many of the same vertices appear as hubs in both the original and the sub-networks. The percentage of common hubs is computed as Common Vertices/Total Vertices in the Original Network. The percentage for core numbers is computed as the ratio of the number of vertices grouped together both in the subgraph and the original network by the total number of vertices in the top 5 core number group of the original network. The higher the value, the better the clustering property and sampling should be maintained. The reduction patterns are similar within the same group, i.e. the GSE5078 or the GSE5140 networks, but changes across groups. The mean clustering coefficients of all the subgraphs are very close to the corresponding original network. For the smaller networks in GSE5078, the sampling technique achieves high reductions from 27% to as much as 53%, while still maintaining nearly 50% or more of the hubs and the core number grouping. For the larger networks in GSE5140, the reduction is around 14% to 26%. The percentage of hubs retained is 50% to 75%.

Combinatorial	Original	Quasi-Chordal Subgraphs with				
Properties	Network	1 Partition	2 Partitions	4 Partitions	8 Partitions	16 Partitions
Middle-Aged Mice (GSE5078)(Vertices 5,549)						
Number of Edges	7,178	5,206(27.4)	4,127(42.5)	3,878(45.9)	3,637(49.3)	**3,362(53.1)**
Mean Clust. Coeff.	.46	.45	.31	.38	.44	.41
High degree vertices	144	83(57)	60(41)	77(53)	80(55)	**92(63)**
Core Numbers	50	30(60)	26(52)	26(52)	28(56)	**44(88)**
Young -Aged Mice (GSE5078)(Vertices 5,549)						
Number of Edges	7,277	4,949(31.9)	4,269(41.3)	4,029(44.6)	**3,657(49.7)**	3,753(48.4)
Mean Clust. Coeff.	.48	.39	.47	.40	.41	.41
High degree vertices	146	73(50)	**106(72)**	96(65)	86(58)	95(65)
Core Numbers	46	26(56)	25(54)	**39(84)**	36(78)	26(56)
Control Group (GSE5140)(Vertices 27,320)						
Number of Edges	29,719	25,281(14.9)	22,284(25)	22,986(22.6)	22,272(25)	**21,898(26.3)**
Mean Clust. Coeff.	.54	.47	.50	.49	.51	.52
High degree vertices	595	368(61)	335(56)	**451(75)**	430(72)	431(72)
Core Numbers	200	34(17)	37(18)	106(53)	112(56)	**106(53)**
Creatine Treated Mice(GSE5140)(Vertices 28,161)						
Number of Edges	33,099	27,278(17.5)	23,867(27.8)	25,268(23.6)	24,719(25.3)	**24,641(25.5)**
Mean Clust. Coeff.	.46	.45	.43	.45	.44	.48
High degree vertices	662	387(58)	360(54)	478(72)	494(74)	**502(76)**
Core Numbers	187	58(31)	45(24)	101(54)	98(52)	**117(62)**

Table 4.1: Comparison of combinatorial properties between original and Chordal subgraphs

In general, the results are better when there are more partitions. This is because by increasing the number of partitions we include more almost-clique structures (by keeping the triangles at border edges), as well as filter out noise.

Combinatorial Properties	Original Network	Random walk Subgraph(1P)
Middle-Aged Mice(GSE5078) (Vertices 5549)		
Number of Edges	7178	2497
Mean Clust. Coeff.	0.27	0.0130
Highest Degree	96	5
Mean Core Numbers	1.77	0.66
Young-Aged Mice(GSE5078) (Vertices 5549)		
Number of Edges	7277	2523
Mean Clust. Coeff.	0.24	0.0098
Highest Degree	116	8
Mean Core Numbers	1.85	0.7
Control Group(GSE5140) (Vertices 27,320)		
Number of Edges	29719	10176
Mean Clust. Coeff.	0.40	0.0209
Highest Degree	84	7
Mean Core Numbers	1.63	0.57
Creatine Treated Mice(GSE5140) (Vertices 28,161)		
Number of Edges	33099	11524
Mean Clust. Coeff.	0.42	0.0218
Highest Degree	150	8
Mean Core Numbers	1.74	0.6

Table 4.2: Comparison of combinatorial properties between the original networks and random walk subgraphs

From Table 4.2, we identified that random walk did not retain any combinatorial properties and values are too low compared to chordal subgraph.

Figure 4.1, 4.2, 4.3, 4.4 plots the degree distribution and the distribution of the average clustering coefficient per degree of the original networks and their chordal subgraphs. As can be seen from the figures, for both metrics, barring slight fluctuations, the subgraphs follow the same pattern as the original network.

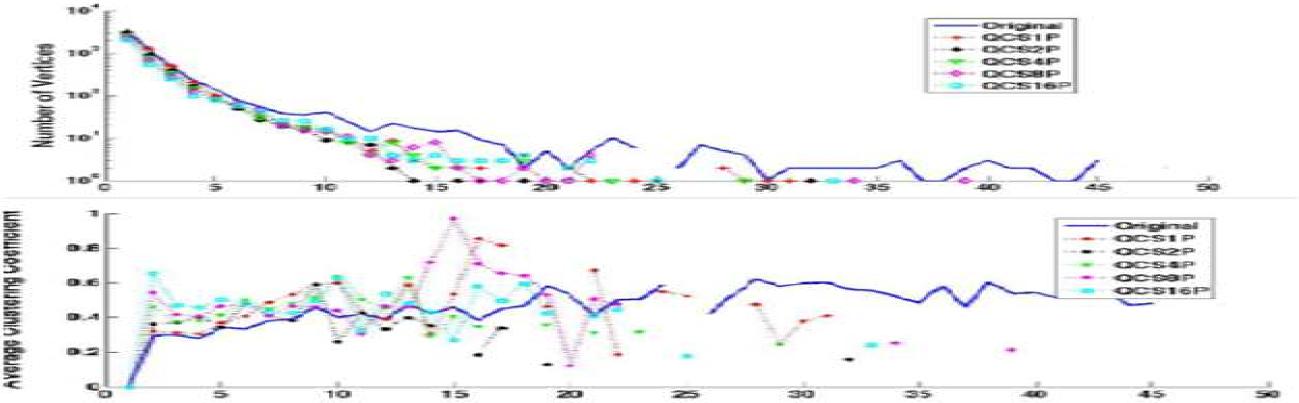

Figure 4.1: Degree distribution and average clustering coefficient of middle aged mice

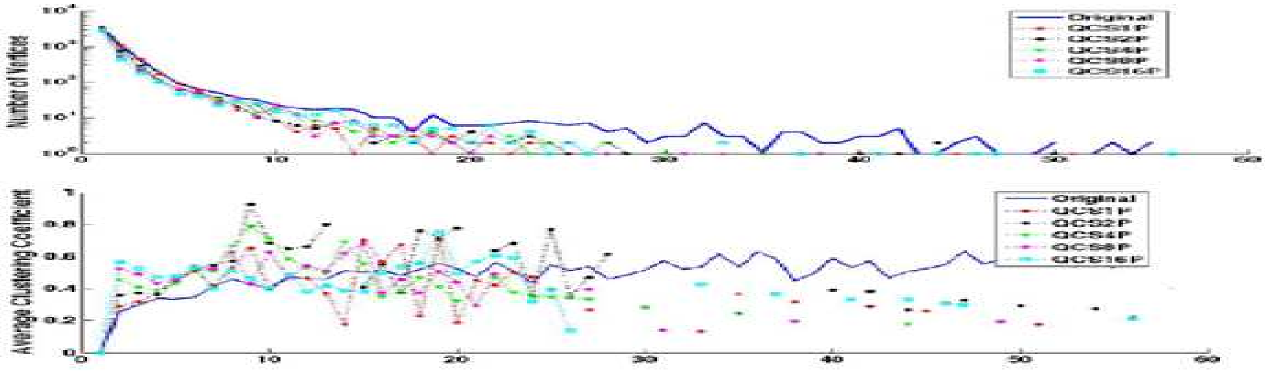

Figure 4.2: Degree distribution and average clustering coefficient of young mice network

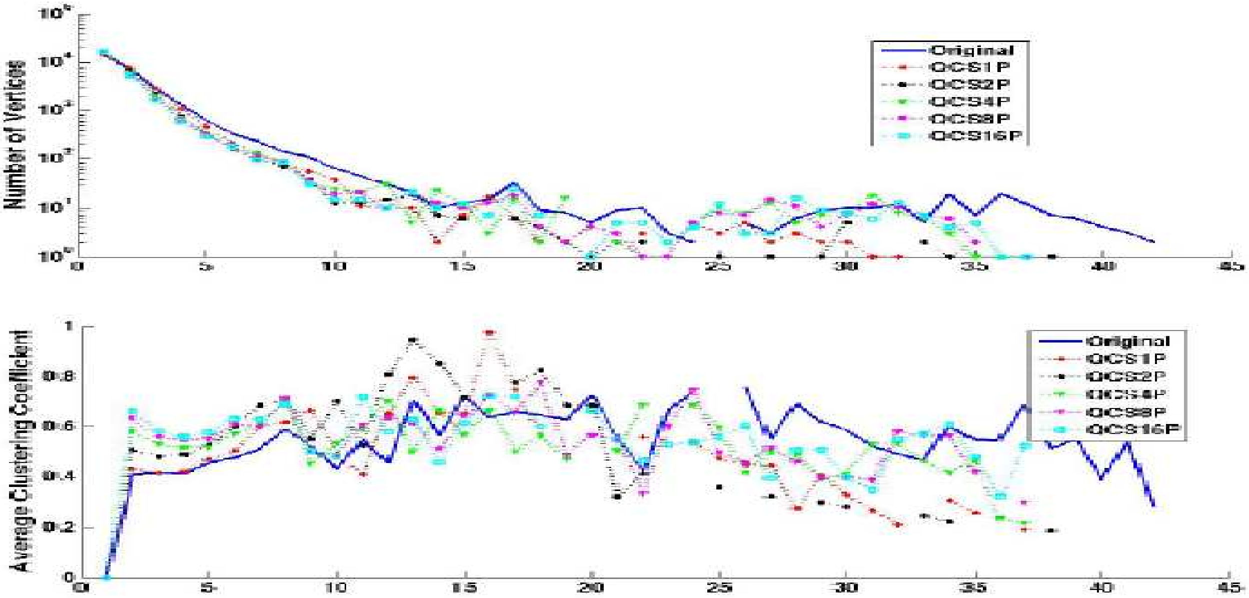

Figure 4.3: Degree distribution and average clustering coefficient of untreated mice

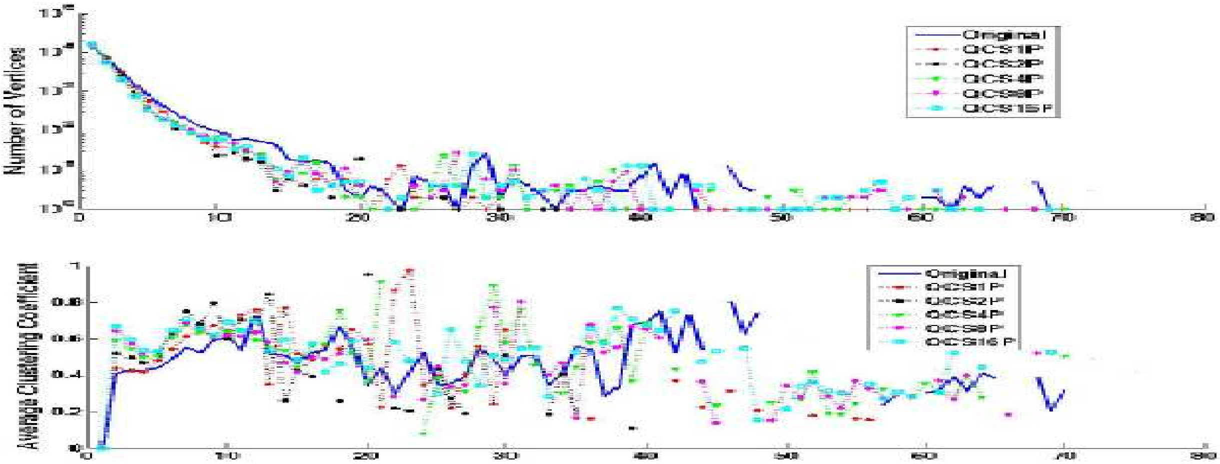

Figure 4.4: Degree distribution and average clustering coefficient of creatine mice

4.2 Analysis of Functional Properties:

We used the Cytoscape plug-in MCODE [26] on the network to identify clusters as groups of genes that are more highly interconnected than they are to the rest of the network. We extracted the top five clusters of the original network and subgraphs and compared the clusters based on maximum common genes in each set. The names of genes in each cluster were given to the PANTHER Classification System (http://www.pantherdb.org/) [27] to identify common molecular functions. Gene Ontology tree is a directed acyclic graph where nodes represent functional descriptive terms and directed edges represent term relationships; a parent-child relationship in the tree indicates that the child term is a more specific function than the parent, thus, the deeper in the tree, the more specialized the terms. Figures lists the most represented Gene Ontology (GO) molecular function terms per cluster as found in the original network and sampled networks on 1,2,4,8 and 16 processors respectively. Similar color within each cluster represents similar functionality.

.

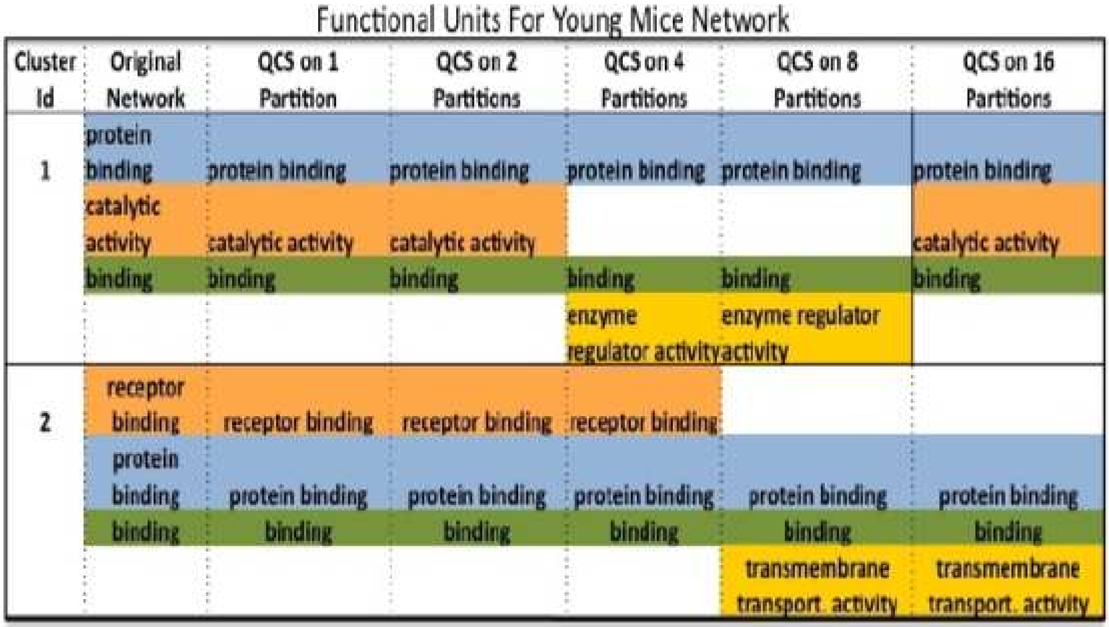

Functional Units For Young Mice Network

Cluster Id	Original Network	QCS on 1 Partition	QCS on 2 Partitions	QCS on 4 Partitions	QCS on 8 Partitions	QCS on 16 Partitions
1	protein binding	protein binding	protein binding	protein binding	protein binding	protein binding
	catalytic activity	catalytic activity	catalytic activity			catalytic activity
	binding	binding	binding	binding	binding	binding
				enzyme regulator activity	enzyme regulator activity	
2	receptor binding	receptor binding	receptor binding	receptor binding		
	protein binding	protein binding	protein binding	protein binding	protein binding	protein binding
	binding	binding	binding	binding	binding	binding
					transmembrane transport. activity	transmembrane transport. activity

Figure 4.5: Comparison of functional units of young mice network.

We define clusters to be overlapped if the same vertex is classified as being in more than one cluster. Except for the young mice network (due to high overlap), most clusters from the original network are present in the subgraphs. There was one small overlap of two clusters in the middle-aged mice network. However, the young mice network exhibited significant overlap of more than two clusters, which affected the comparison of the functional units. We conjecture that was because the gene pathways of the young mice are in a more fluid and volatile state than the more fixed gene pathways of older mice.

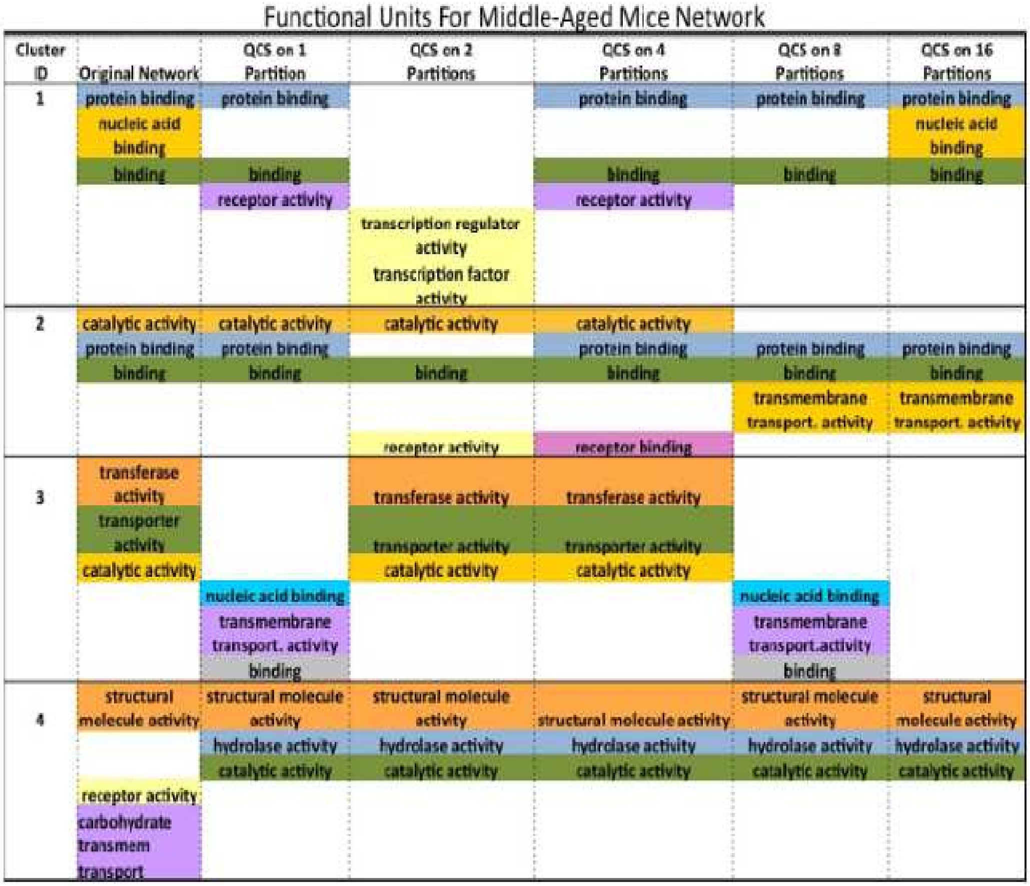

Functional Units For Middle-Aged Mice Network

Cluster ID	Original Network	QCS on 1 Partition	QCS on 2 Partitions	QCS on 4 Partitions	QCS on 8 Partitions	QCS on 16 Partitions
1	protein binding	protein binding		protein binding	protein binding	protein binding
	nucleic acid binding					nucleic acid binding
	binding	binding		binding	binding	binding
		receptor activity		receptor activity		
			transcription regulator activity transcription factor activity			
2	catalytic activity	catalytic activity	catalytic activity	catalytic activity		
	protein binding	protein binding		protein binding	protein binding	protein binding
	binding	binding	binding	binding	binding	binding
					transmembrane transport. activity	transmembrane transport. activity
			receptor activity	receptor binding		
3	transferase activity		transferase activity	transferase activity		
	transporter activity		transporter activity	transporter activity		
	catalytic activity		catalytic activity	catalytic activity		
		nucleic acid binding			nucleic acid binding	
		transmembrane transport. activity			transmembrane transport.activity	
		binding			binding	
4	structural molecule activity	structural molecule activity	structural molecule activity	structural molecule activity	structural molecule activity	structural molecule activity
		hydrolase activity	hydrolase activity	hydrolase activity	hydrolase activity	hydrolase activity
		catalytic activity	catalytic activity	catalytic activity	catalytic activity	catalytic activity
	receptor activity					
	carbohydrate transmem transport					

Figure 4.6: Comparison of functional units of the networks of middle aged datset

The results show that sampling from the larger networks from the GSE5140(Untreated Mice Network and Creatine Mice Network) match to more functional units than the smaller networks, and the matching improves with larger number of partitions. We also note that several subgraphs show common functional units (such as in cluster 3 of the middle aged mice and in cluster 1 of the creatine treated mice) which are not present in the original cluster. We conjecture that the removal of noisy edges has exposed these functional units previously hidden in the original network.

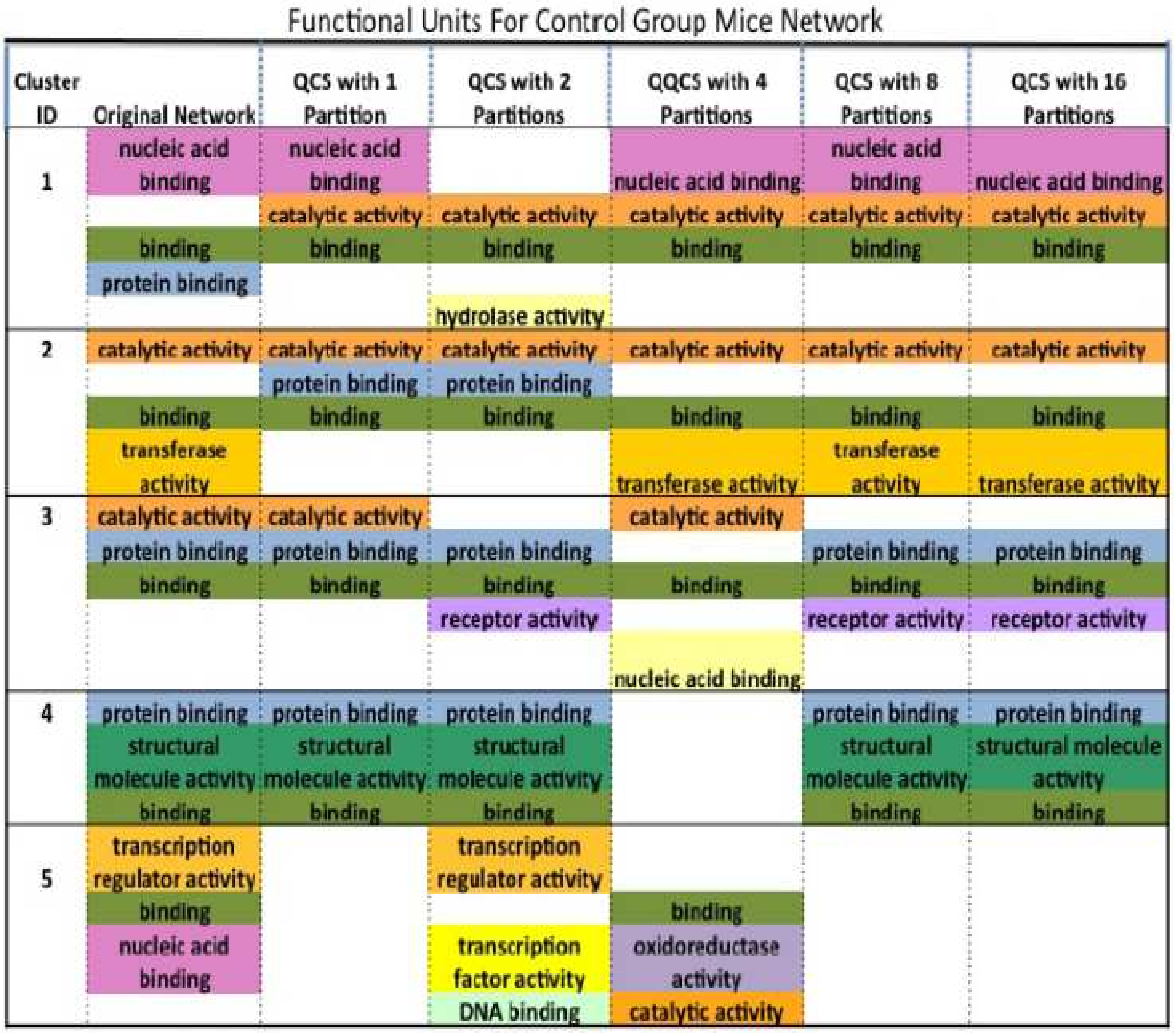

Functional Units For Control Group Mice Network

Cluster ID	Original Network	QCS with 1 Partition	QCS with 2 Partitions	QQCS with 4 Partitions	QCS with 8 Partitions	QCS with 16 Partitions
1	nucleic acid binding	nucleic acid binding		nucleic acid binding	nucleic acid binding	nucleic acid binding
		catalytic activity	catalytic activity	catalytic activity	catalytic activity	catalytic activity
	binding	binding	binding	binding	binding	binding
	protein binding					
			hydrolase activity			
2	catalytic activity	catalytic activity	catalytic activity	catalytic activity	catalytic activity	catalytic activity
		protein binding	protein binding			
	binding	binding	binding	binding	binding	binding
	transferase activity			transferase activity	transferase activity	transferase activity
3	catalytic activity	catalytic activity		catalytic activity		
	protein binding	protein binding	protein binding		protein binding	protein binding
	binding	binding	binding	binding	binding	binding
			receptor activity		receptor activity	receptor activity
				nucleic acid binding		
4	protein binding	protein binding	protein binding		protein binding	protein binding
	structural molecule activity	structural molecule activity	structural molecule activity		structural molecule activity	structural molecule activity
	binding	binding	binding		binding	binding
5	transcription regulator activity		transcription regulator activity			
	binding			binding		
	nucleic acid binding		transcription factor activity	oxidoreductase activity		
			DNA binding	catalytic activity		

Figure 4.7: Comparison of functional units of untreated mice dataset

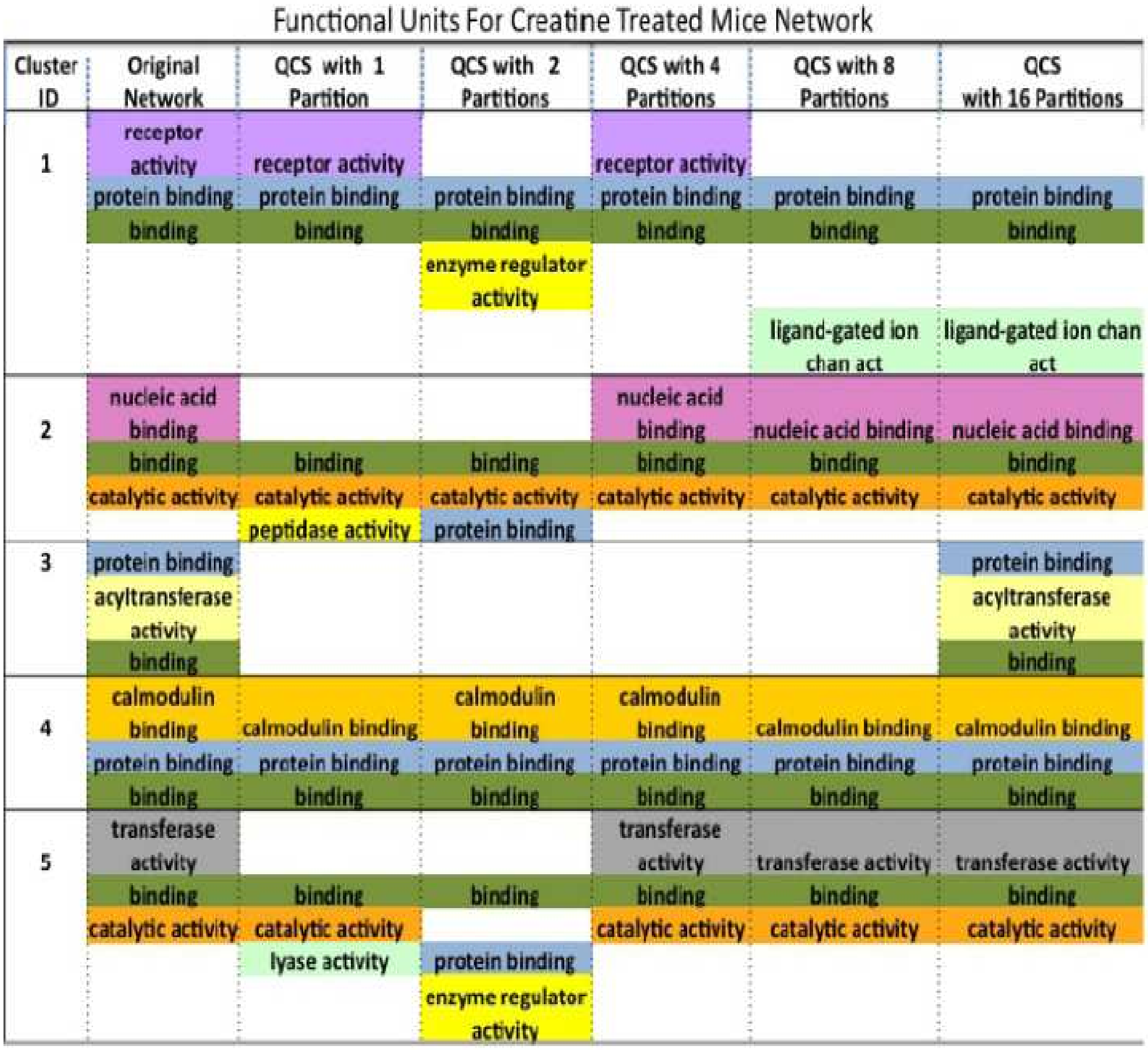

Functional Units For Creatine Treated Mice Network

Cluster ID	Original Network	QCS with 1 Partition	QCS with 2 Partitions	QCS with 4 Partitions	QCS with 8 Partitions	QCS with 16 Partitions
1	receptor activity	receptor activity		receptor activity		
	protein binding	protein binding	protein binding	protein binding	protein binding	protein binding
	binding	binding	binding	binding	binding	binding
			enzyme regulator activity			
					ligand-gated ion chan act	ligand-gated ion chan act
2	nucleic acid binding			nucleic acid binding	nucleic acid binding	nucleic acid binding
	binding	binding	binding	binding	binding	binding
	catalytic activity	catalytic activity	catalytic activity	catalytic activity	catalytic activity	catalytic activity
		peptidase activity	protein binding			
3	protein binding					protein binding
	acyltransferase activity					acyltransferase activity
	binding					binding
4	calmodulin binding	calmodulin binding	calmodulin binding	calmodulin binding	calmodulin binding	calmodulin binding
	protein binding	protein binding	protein binding	protein binding	protein binding	protein binding
	binding	binding	binding	binding	binding	binding
5	transferase activity			transferase activity	transferase activity	transferase activity
	binding	binding	binding	binding	binding	binding
	catalytic activity	catalytic activity		catalytic activity	catalytic activity	catalytic activity
		lyase activity	protein binding			
			enzyme regulator activity			

Figure 4.8: Comparison of functional units of creatine treated mice dataset.

4.2.1 Analysis of Different Ordering:

We extend the research and compare the effectiveness of chordal graph sampling based on Breadth First Search (BFS) and Reverse Cuthill Mckee (RCM) [10] ordering .It's because ordering of the vertices in the parallel algorithm, play a significant role in determining the size and quality of the maximal quasi-chordal graph.

BFS ordering is based on a level by level traversal of the graph, where the level of a vertex is its shortest distance from the starting vertex. BFS assures that the vertices in the same connected graph component will be processed together.RCM ordering, in addition to accessing connected components, ensures that closely connected groups of vertices are placed together. RCM ordering is implemented by reversing the vertex order obtained from a BFS search, with the constraint that the starting vertex is a peripheral vertex [2].

Each column in the Figure 12 and 13 denotes clusters and corresponding enrichment score found in the original network and through sampled networks on 1, 2, 4, 8, 16 and 32 processors respectively. Enrichment for a Gene Ontology term can be described as the ratio of the number of genes in the cluster with the specified term (c) to the number of genes in the cluster (n), divided by the ratio of the number of genes in the entire genome with the specified term (C) to the total number of genes in the tested genome (N). The formal equation to identify enrichment, then, is $E = (c/n)/(C/N)$. The higher the enrichment score, the better.

In the young mouse dataset, the original network had 2 of the top clusters enriched in with GO terms associated with Development and Transport. Clusters matching to these functionalities were also found in the sampling method using BFS ordering (Figure 4.9). The BFS results identified the Development cluster (cluster 3) for each number of partitions (1, 2, 4, 8, 16, and 32) whereas the Transport cluster (cluster 5) was only identified on the sample using one processor. The BFS method also helped in discovery of new clusters which were enriched in metabolism (cluster 1), development (clusters 2 and 3), and transport (cluster 4).

In the case of RCM ordering (Figure 4.10), Metabolism enriched cluster (cluster 6) was preserved from the original network (for sampling in one processor and two processors). New clusters identified were enriched in transport (cluster 2), metabolism (cluster 1 and 3), and development (cluster 4). Compared to the BFS results (Figure 2), these results were more functionally specific, suggesting that RCM may retain knowledge better than BFS.

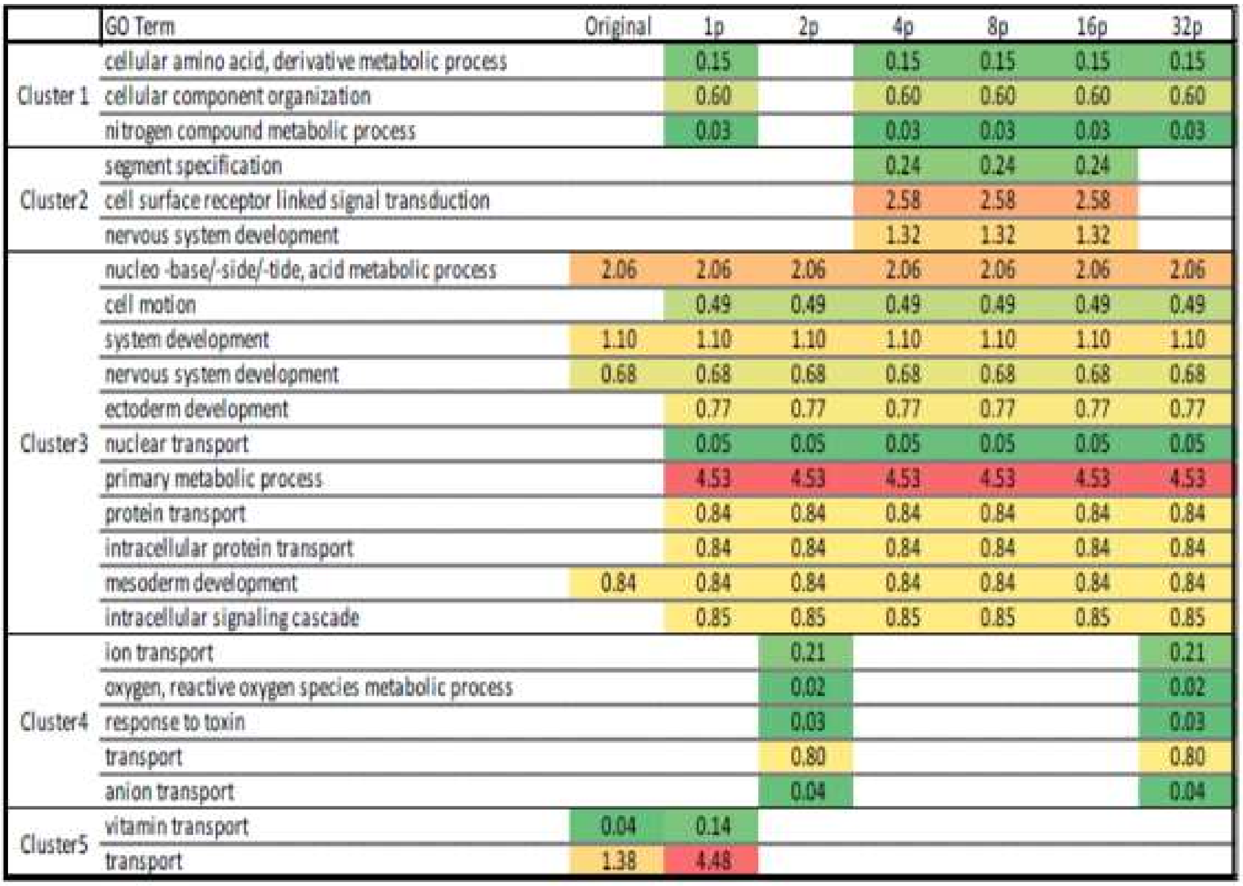

	GO Term	Original	1p	2p	4p	8p	16p	32p
Cluster 1	cellular amino acid, derivative metabolic process		0.15		0.15	0.15	0.15	0.15
	cellular component organization		0.60		0.60	0.60	0.60	0.60
	nitrogen compound metabolic process		0.03		0.03	0.03	0.03	0.03
Cluster2	segment specification				0.24	0.24	0.24	
	cell surface receptor linked signal transduction				2.58	2.58	2.58	
	nervous system development				1.32	1.32	1.32	
Cluster3	nucleo -base/-side/-tide, acid metabolic process	2.06	2.06	2.06	2.06	2.06	2.06	2.06
	cell motion		0.49	0.49	0.49	0.49	0.49	0.49
	system development	1.10	1.10	1.10	1.10	1.10	1.10	1.10
	nervous system development	0.68	0.68	0.68	0.68	0.68	0.68	0.68
	ectoderm development		0.77	0.77	0.77	0.77	0.77	0.77
	nuclear transport		0.05	0.05	0.05	0.05	0.05	0.05
	primary metabolic process		4.53	4.53	4.53	4.53	4.53	4.53
	protein transport		0.84	0.84	0.84	0.84	0.84	0.84
	intracellular protein transport		0.84	0.84	0.84	0.84	0.84	0.84
	mesoderm development	0.84	0.84	0.84	0.84	0.84	0.84	0.84
	intracellular signaling cascade		0.85	0.85	0.85	0.85	0.85	0.85
Cluster4	ion transport			0.21				0.21
	oxygen, reactive oxygen species metabolic process			0.02				0.02
	response to toxin			0.03				0.03
	transport			0.80				0.80
	anion transport			0.04				0.04
Cluster5	vitamin transport	0.04	0.14					
	transport	1.38	4.48					

Figure 4.9: The gene functionality of clusters for the young mouse network with BFS ordering. Enrichment scores are colored from low (green) to high (red). Spaces with no enrichment means that for that number of partitions, there was no cluster found for that partition. Number of conserved clusters: 1. Number of clusters with additional genes: 1. Number of new clusters in sampled networks: 3.

Our results indicate that RCM had more matches to original GO clusters identified, indicating that lowering the bandwidth of the corresponding matrix can help in obtaining more clustered regions.

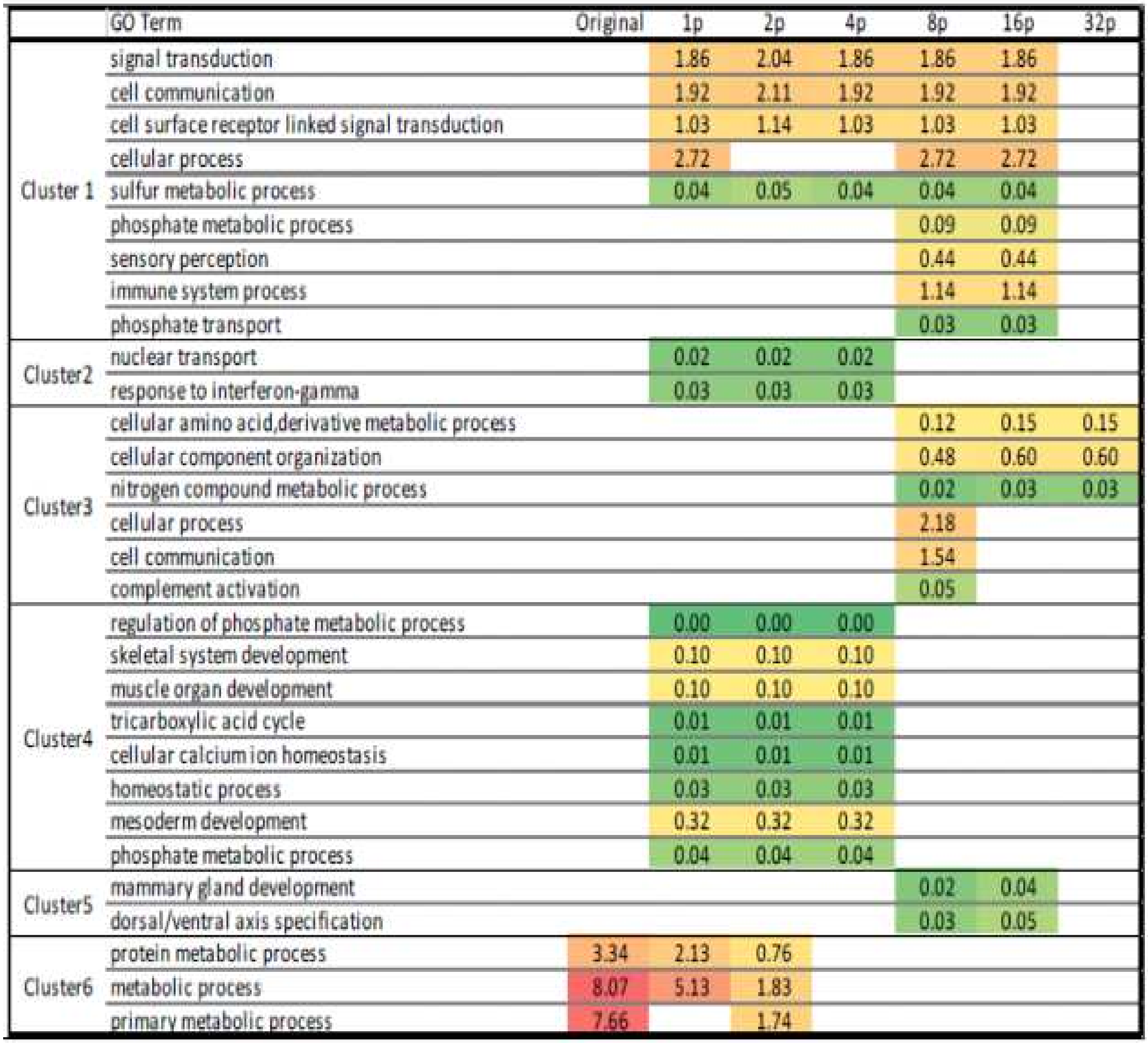

	GO Term	Original	1p	2p	4p	8p	16p	32p
Cluster 1	signal transduction		1.86	2.04	1.86	1.86	1.86	
	cell communication		1.92	2.11	1.92	1.92	1.92	
	cell surface receptor linked signal transduction		1.03	1.14	1.03	1.03	1.03	
	cellular process		2.72			2.72	2.72	
	sulfur metabolic process		0.04	0.05	0.04	0.04	0.04	
	phosphate metabolic process					0.09	0.09	
	sensory perception					0.44	0.44	
	immune system process					1.14	1.14	
	phosphate transport					0.03	0.03	
Cluster2	nuclear transport		0.02	0.02	0.02			
	response to interferon-gamma		0.03	0.03	0.03			
Cluster3	cellular amino acid,derivative metabolic process					0.12	0.15	0.15
	cellular component organization					0.48	0.60	0.60
	nitrogen compound metabolic process					0.02	0.03	0.03
	cellular process					2.18		
	cell communication					1.54		
	complement activation					0.05		
Cluster4	regulation of phosphate metabolic process		0.00	0.00	0.00			
	skeletal system development		0.10	0.10	0.10			
	muscle organ development		0.10	0.10	0.10			
	tricarboxylic acid cycle		0.01	0.01	0.01			
	cellular calcium ion homeostasis		0.01	0.01	0.01			
	homeostatic process		0.03	0.03	0.03			
	mesoderm development		0.32	0.32	0.32			
	phosphate metabolic process		0.04	0.04	0.04			
Cluster5	mammary gland development					0.02	0.04	
	dorsal/ventral axis specification					0.03	0.05	
Cluster6	protein metabolic process	3.34	2.13	0.76				
	metabolic process	8.07	5.13	1.83				
	primary metabolic process	7.66		1.74				

Figure 4.10: The gene functionality of clusters for the young mouse network with RCM ordering. Enrichment scores are colored from low (green) to high (red). Spaces with no enrichment means that for that number of partitions, there was no cluster found for that partition. Number of conserved clusters: 1. Number of new clusters in sampled networks: 6.

Additionally, both methods performed exceptionally at identifying novel clusters within networks, which indicates that sampling based on identifying quasi chordal subgraphs can indeed eliminate poorly connected edges, which form noise in the network. RCM method had higher conservation of novel cluster identification than BFS across number of partitions, suggesting that it may be more stable than the BFS method.

4.2.2 Analysis of Quality of Clusters:

Resulting cluster of both original network and sampled subgraphs are annotated and scored and ranked according to true biological networks. All clusters from original networks are compared to all clusters from sampled networks based on the following metrics: (i) node overlap, (ii) edge overlap, (iii) biological relevance of clusters in the original versus the sampled networks, (iv) number of known (found in the original network) and new (not found in the original network) clusters identified.

We define some terms that is useful in understanding the subsequent explanation of analysis of clusters.

Cluster Annotation and Scoring: For each edge *e* connecting nodes *n1* and *n2* in some cluster *C*, the terms associated with genes represented by nodes *n1* and *n2* are identified and mapped onto the GO biological process tree. Then the deepest common parent/ancestor (DCP) of nodes *n1* and *n2* is identified and used to annotate edge *e*. Scoring is performed using a measure of DCP depth (distance from the ROOT node to the DCP) and term breadth (length of the shortest path from term 1 and term 2) where the final score of edge e is equal to DCP depth – term breadth[28]. Clusters are scored by taking the average edge enrichment score (AEES) over all edges in the cluster and function is annotated using the most common/dominating term(s) within the cluster. Edges that represent true relationships will be deep in the tree and closer to each other, so the higher the edge score, the better. In addition, scores at or below 0 are more likely to represent noise or coincidental relationships.

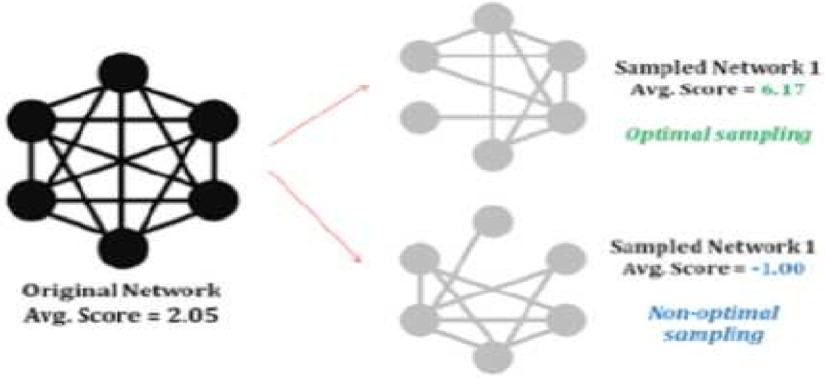

Figure 4.11: Example of how network sampling can positively or negatively affect the average edge enrichment score of a cluster by removing different sets of edges.

Vertex Ordering: The size of maximal chordal graph depends on the order in which vertices are accessed. To check whether analysis of gene functionality get affected by ordering , we permuted the original network according to four different ordering as follows.

1. Natural Order: This is the original order in which the vertices were arranged in the network. This order is generally based on the nomenclature of the genes, such as arranging the genes in alphabetical order

2. High Degree Order: The vertices are arranged in descending order of degree. The ones with the higher degree are likely to be processed first

*3. Low Degree Order***:** The vertices are arranged in ascending order of degree. The ones with the lowest degree are likely to be processed first

4. Reverse Cut hill McKee (RCM Order): This ordering ensures that closely connected group of vertices are placed together.

Cluster Overlap: We use the following measures to define sensitivity and specificity of our filters as follows.

1. High AEES, High overlap (True Positive TP): Clusters that have a high AEES and have a high (>50%) node or edge overlap indicates clusters that were found in the original network and the sampled network, and the cluster has biological meaning.

2. *Low AEES, High overlap (False Positive FP):* Clusters that have a low AEES and have a high (>50%) node or edge overlap indicates clusters that were found in the original network and the sampled network, but the cluster likely has no biological meaning.

3. *High AEES, Low overlap (False Negative FN):* Clusters that have a high AEES and have a low (<50%) node or edge overlap indicates clusters that were *not* found in the original network but were present in the sampled network, and have biological meaning. These clusters tend to be small and less dense and are only uncovered when noise is removed; hence they are hidden in the original network.

4. *Low AEES, Low overlap (True Negative TN):* Clusters that have a low AEES and have a low (<50%) node or edge overlap indicates clusters that were *not* found in the original network but were present in the sampled network, and likely have no biological meaning.

By dividing the graph into equal quadrants, we can identify TP, FP, FN and TN counts in figure 4.12.

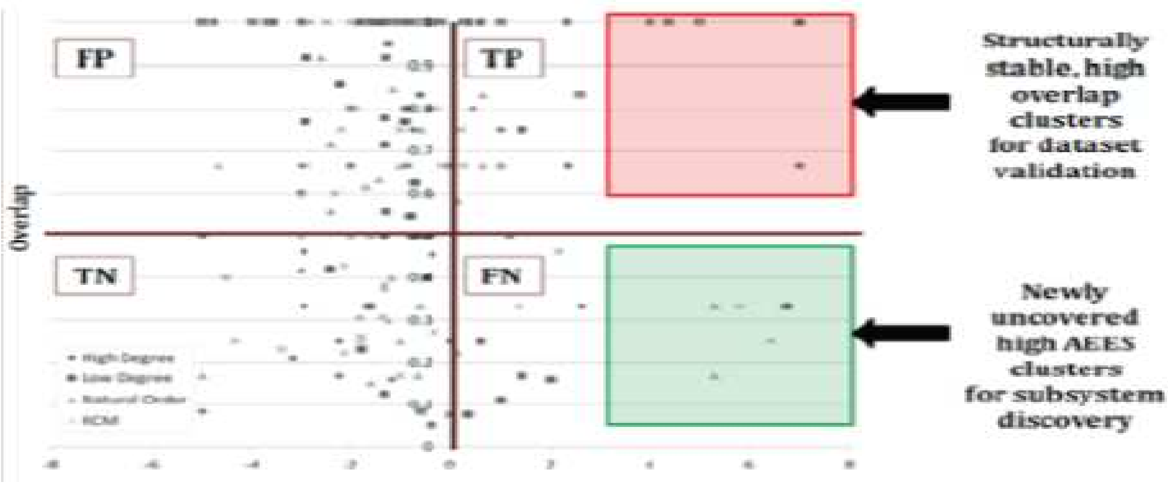

Figure 4.12: Example of how to identify the likely biologically meaningful clusters

Red box highlights clusters with high AEES scores that were found in both original and clustered networks; the green box highlights clusters with high AEES scores that were found in the original network but were ranked higher in filtered networks. Using these measures, we can define Sensitivity (TP/(TP+FN)) and Specificity (TN/(TN+FP))for each filter to identify which (if any) orderings are optimal compared to the others.

Node and Edge Overlap:

We now analyze the quality of the clusters in each network as obtained by the filters.

Figure 4.13 depicts the overlap of filtered clusters with original clusters in terms of percentage of node overlap and percentage of edge overlap. Each point represents a cluster found for a particular filter that had some overlap with a cluster in the original network. Points lying near the right and the top have higher overlap. Although the filtering method removes edges, we still found some filters to leave complete clusters (100% edge and node overlap) from the original.

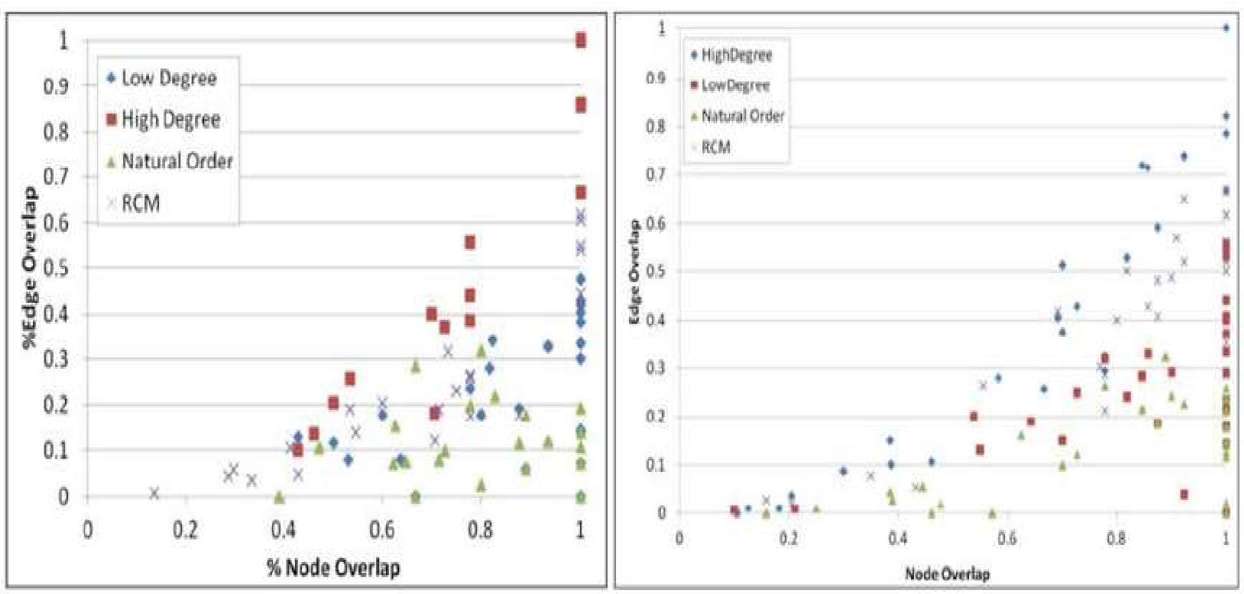

Figure 4.13: Node and edge overlap for original vs. sampled networks , untreated scores (left) and creatine scores(right)

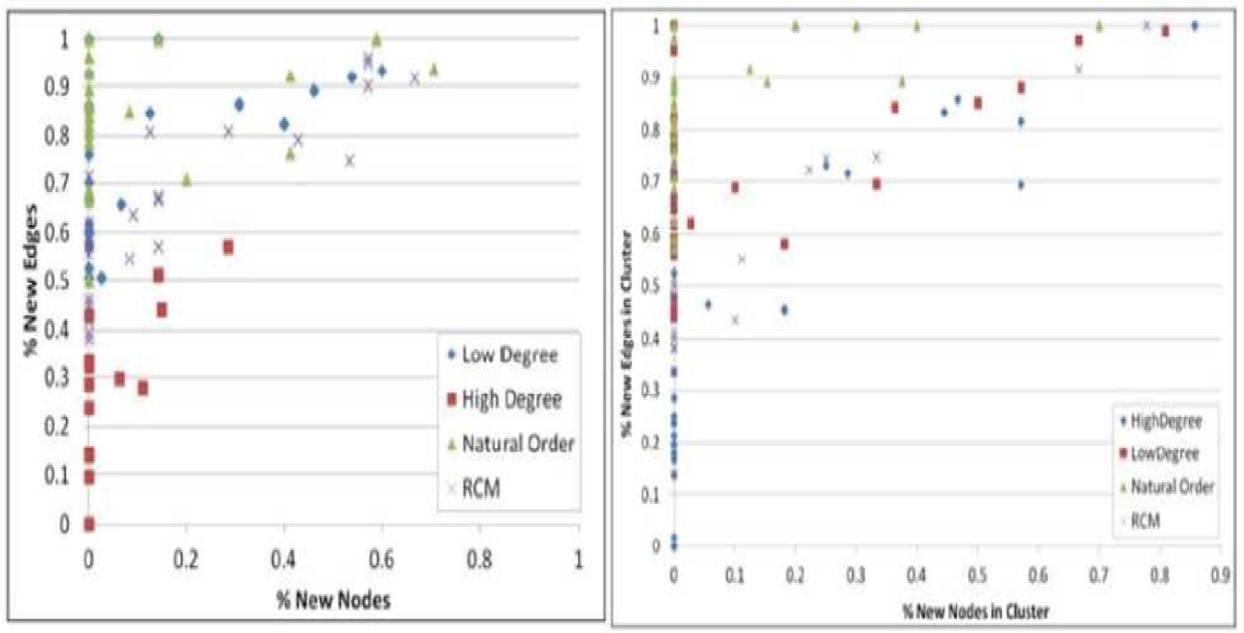

Figure 4.14: Newly discovered nodes and edges for original vs. sampled networks , untreated scores (left) and creatine scores(right)

Figure 4.14 depicts clusters that were not found in original network. Points lying near the left and the bottom have less overlap. While these figures note the density of discovered clusters, it remains to be seen whether these newly found clusters are actually biologically relevant. Among the orderings we see that high and low degree orderings retain the maximum number of clusters from the original networks and natural order seems to be the best identifier of new clusters, followed by RCM.

We observe that many points on the graph lie on the same coordinates indicating that the despite different orderings chordal based filters retain many important clusters. Therefore our algorithms have minimal overall impact on the process of obtaining biologically relevant clusters.

Next, we examine the sensitivity and specificity of our ordering methods from TP, FP, FN and TN. We see in Figure 4.15 that identifying clusters by percentage of node overlap returns a high sensitivity and low specificity, that is we find many meaningful clusters but also find many non meaningful clusters. Edge overlap shows the opposite; specifically that using edge overlap to define a cluster match from original to filter allows us to find clusters that are likely to be noise, although the reasoning behind this is not clear.

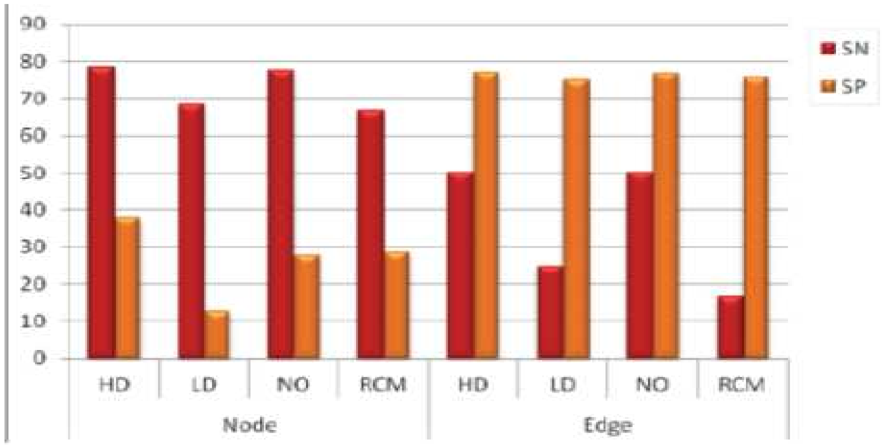

Figure 4.15: Sensitivity and specificity of filters for node and edge overlap.

Finally, we see that filters can improve on AEE score of original clusters and allow the true function to stand out. Figure 4.16. A denotes entire cluster represents cluster 18 of original UNT network, AEES score of 2.33. Red nodes and edges represent the sampled UNT High Degree cluster #10 with AEES score of 4.17, an improvement of almost 2.00 enrichment points on average. Figure 4.16.B represents the resulting filtered cluster was annotated involvement in apoptotic function; three nodes have been confirmed as having roles in apoptosis via multiple sources (MGI, NCBI, GO, etc.), two nodes have been confirmed in the GO tree and in literature, and two remaining in the filtered network (and additional two in the original network) have not previously been identified as having apoptotic function. By filtering the sample, two nodes with no apoptotic function are removed and the cluster's true function is revealed. Whereas figure 4.16.C denotes the UNT HD cluster #10 with edges enriched in apoptosis as the DCP highlighted in purple dashed lines.

This original cluster did not stand out in the ranked list but stood out in all 4 filtered networks as a high AEE scored cluster with high overlap (66.7% node overlap, 28% edge overlap) to original and was found to be involved in regulation of apoptosis in the UNT network. Apoptosis is a critical process for normally functioning cells; when apoptosis is not regulated appropriately it can result in uncontrolled cell growth (cancer) or too much cell death (necrosis).

Our experiments showed that random walk filtered networks find no clusters at all. The random walk filter does not identify subsystems/graphs within the network at all, in that there are not enough edges retained using the random walk method to identify very dense groups of nodes. Thus, no clusters are identified via the random walk method.

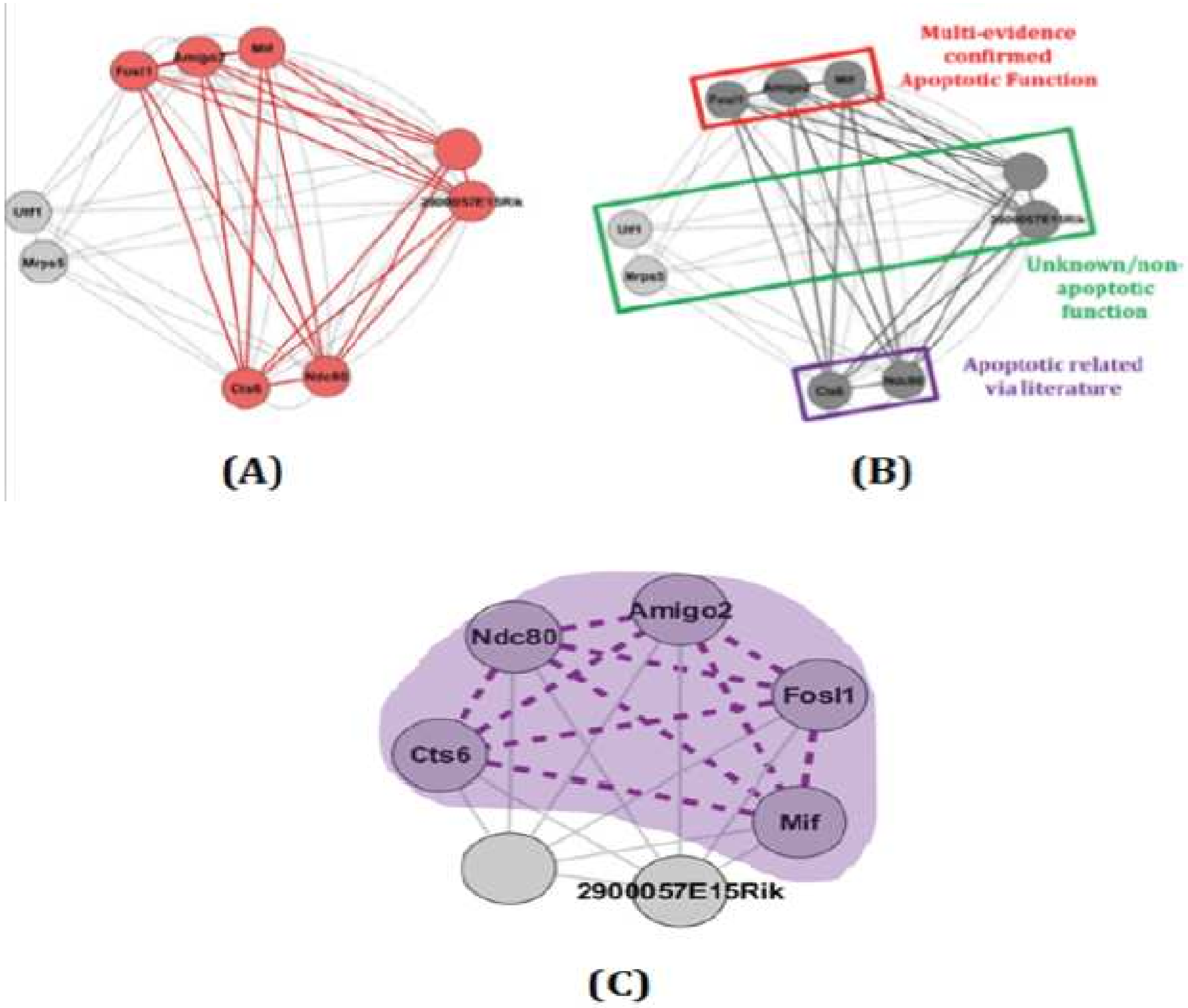

Figure 4.16: Example of how filtering impacts a cluster.

4.3 Analysis of Parallel Results:

We demonstrate the scalability of our parallel chordal graph based sampling algorithm. Our experiments were performed on the Firefly Cluster at the Holland Computing Center. Firefly is a Linux-based system comprising of AMD quad- and dual-core processors. Our implementation was based on a distributed memory approach using MPI. We compared the scalability of the following three sampling algorithms: (i) chordal graph based sampling using communication, (ii) chordal graph based sampling without communication, and (iii) random walk.

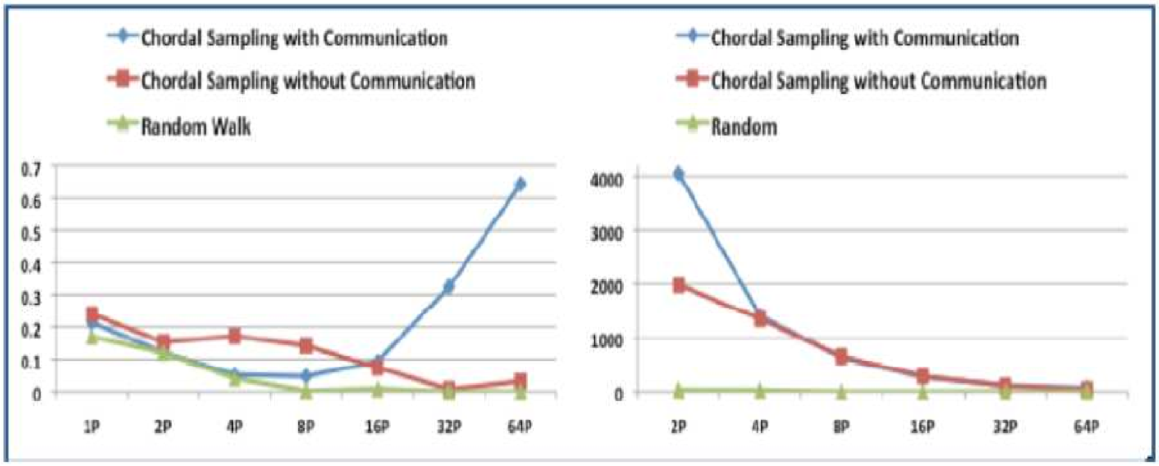

Figure 4.17: Scalability of sampling algorithms for a dataset with 5,348 vertices and 7,277 edges(Above) and dataset with 27,896 vertices and 30,296 edges(Below)

As expected the random walk filter is the most scalable of all and also the fastest. Chordal sampling without communication is also very scalable and takes less time than the version with communication. The scalability for chordal sampling with communication deteriorates for small graphs and for large graphs the time taken can be as much as twice that required for the algorithm without communication.

We compare the results of the original networks to two different types of the new chordal based filter: sequential (1P) and multiple processors (64P) to show that parallel implementation of our method do not negatively affect cluster identification. We see that in Figure 4.18 (left) the method at 64P is comparable to the method at 1P, although the clusters found at 64P have better node overlap (no clusters have less that 40% node overlap) and moderate edge overlap (no better than 50% edge overlap with original clusters). Each point represents a cluster found in the original network that overlaps with a cluster found in the filtered network.

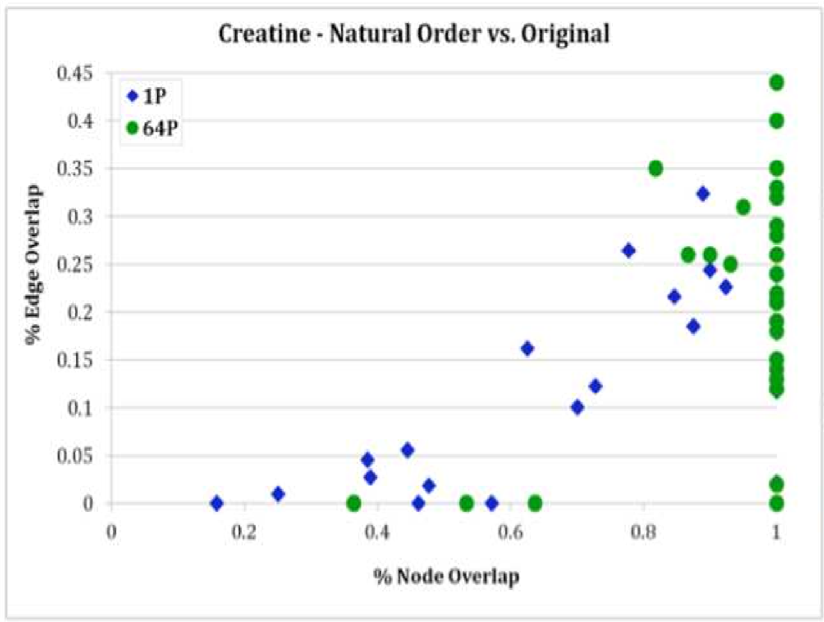

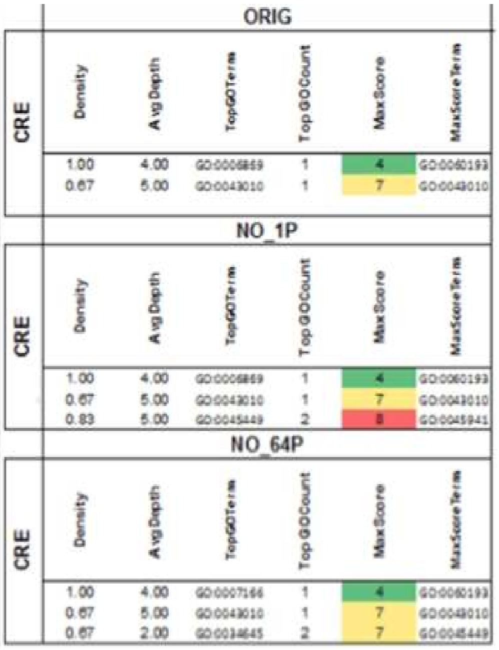

ORIG

CRE	Density	Avg Depth	TopGOTerm	Top GOCount	MaxScore	MaxScoreTerm
	1.00	4.00	GO:0006869	1	4	GO:0060193
	0.67	5.00	GO:0043010	1	7	GO:0043010

NO_1P

CRE	Density	Avg Depth	TopGOTerm	Top GOCount	MaxScore	MaxScoreTerm
	1.00	4.00	GO:0006869	1	4	GO:0060193
	0.67	5.00	GO:0043010	1	7	GO:0043010
	0.83	5.00	GO:0045449	2	8	GO:0045941

NO_64P

CRE	Density	Avg Depth	TopGOTerm	Top GOCount	MaxScore	MaxScoreTerm
	1.00	4.00	GO:0007166	1	4	GO:0060193
	0.67	5.00	GO:0043010	1	7	GO:0043010
	0.67	2.00	GO:0034645	2	7	GO:0045449

Figure 4.18: Parallel results for Creatine Natural Order filter.

Figure 4.18(Right) represents Clusters with AEES scores >3.0 found in original, 1P and 64P networks. The average depth is the AEES score, and Max Score represents the deepest term represented in the cluster.

Chapter 5
Conclusion

We developed and implemented a scalable parallel graph sampling algorithms based on extracting the maximal chordal subgraphs from large networks. We showed that our sampled subgraphs retain most of the combinatorial and functional properties of the original network. We present the detailed analysis of clusters obtained by comparing the random filter method and also chordal graph with different permutations of network. Our analysis show that maximal chordal subgraphs will maintain or improve upon the biological information contained within the highly dense subgraphs. Reported results also show that our parallel implementation is scalable and the analysis results are not significantly affected by data distribution and ordering of vertices. Thus, our method tries to find the best description of the network being analyzed, no matter what kind of network.

As a part of future work, we can investigate the impact of implementing other methods for reducing noise in the network, such as identifying Steiner trees or Hypergraph and also continue the network sampling on weighted networks and on dynamic evolving networks.

References:

[1] J. C. Miller and J. M. Hyman. Effective vaccination strategies for realistic social networks. Physica A.386,780-785(2007).

[2] K. Voevodski, S. H. Teng, and Y. Xia. Finding local communities in protein networks BMC Bioinformatics,10, 297(2009).

[3] R. Yokomori, H. Siy, M. Noro, and K. Inoue. Assessing the Impact of Framework Changes Using Component Ranking. International Conference on Software Maintenance. ICSM '09.2009.

[4] D. A. Bader, G. Cong. A Fast, Parallel Spanning Tree Algorithm for Symmetric Multiprocessors.18th International Parallel and Distributed Processing Symposium. IPDPS'04.

[5] G. Cong, G. Almasi, V. Saraswat. A Fast PGAS Implementation of Distributed Graph Algorithms. Proceedings of the 2010 ACM/IEEE International Conference for High Performance Computing, Networking, Storage and Analysis, SC’10. 2010.

[6] V. Agarwal, F. Petrini, D. Pasetto and D. A. Bader. Scalable Graph Exploration on Multicore Processors. Proceedings of the 2010 ACM/IEEE International Conference for High Performance Computing, Networking, Storage and Analysis. SC’10. 2010.

[7] J. Leskovec and C. Faloutsos. Sampling from large graphs. Proceedings of the 12th ACM SIGKDD international conference on Knowledge discovery and data mining, KDD’06. 2006.

[8] V. Krishnamurthy, M. Faloutsos, J.-H. Chrobak, M. Cui, L. Lao, and A. G. Percus. Sampling large internet topologies for simulation purposes. Computer Networks 51, 2007, 4284–4302.

[9] J. Leskovec, J. Kleinberg, C. Faloutsos. Graphs over time: densification laws, shrinking diameters and possible explanations. Proceedings of the eleventh ACM SIGKDD international conference on Knowledge discovery in data mining, KDD’05. 2005.

[10] J. L. Gross, J. Yellen. Handbook of Graph Theory and Applications, CRC Press, 2004.

[11] D.rafiei ,s.curial ,Effectively Visualizing Large Networks Through Sampling, In Visualization,2005

[12] A.Gilbert, K. Levchenko ,Compressing Network Graphs, In LinkKDD,2004

[13] Mashaghi.A et al, Investigation of a Protein Complex Network, European Physical Journal,B41(1):113-121

[14]Arun.S.Maiya and Tanya.Y.Berger Wolf. Benefits of Bias: Towards better Characterization of network sampling.Proceedings of KDD'11.2011

[15] A. Rasti, M. Torkjazi, R. Rejaie, N. Duffield, W. Willinger, D. Stutzbach, Respondent-driven sampling for characterizing unstructured overlays, INFOCOM 2009. pp. 2701–2705.

[16] A. Miranda, L. Garcia, A. Carvalho, and A. Lorena, Use of classification algorithms in noise detection and elimination. Hybrid Artificial Intelligence Systems, Lecture Notes in Computer Science, 5572. 2009, pp. 417–424.

[17] G. L. Libralon, A. Carvalho, and A. C. Lorena, Preprocessing for noise detection in gene expression classification data. Journal of the Brazilian Computer Society 15.2009, 3 –11.

[18] P. M. Dearing, D. R. Shier and D. D. Warner, Maximal Chordal Subgraphs, Discrete Applied Mathematics.20, 3,1988. 181-190.

[19] N. S. Watson-Haigh, H. N. Kadarmideen, A. Reverter, Pcit: An r package for weighted gene co-expression networks based on partial correlation and information theory approaches, Bioinformatics(Oxford, England) 26 (3) (2010) 411–413.

[20] W. J. Ewens, G. R. Grant, Statistical methods in bioinformatics (Second Edition ed.), New York, NY: Springer, 2005.

[21] M. Mutwil, U. B., S. M., A. Loraine, O. Ebenhoh, S. Persson, Assembly of an interactive correlation network for the arabidopsis genome using a novel heuristic clustering algorithm, Plant Physiology 152 (1) (2010) 29–43.

[22] A. L. Barabasi, Z. N. Oltvai, Network biology: Understanding the cell's functional organization, Nature Reviews.Genetics 5 (2) (2004) 101–113.

[23] Verbitsky, M, Yonan, AL, Malleret, G, Kandel, ER, Gilliam, T C, & Pavlidis, P. (2004). Altered hippocampal transcript profile accompanies an age-related spatial memory deficit in mice. Learning & Memory (Cold Spring Harbor, N.Y.), 11(3), 253-260.

[24] Bender A, Beckers J, Schneider I, Hölter SM et al. Creatine improves health and survival of mice. Neurobiol Aging 2008 Sep;29(9):1404-11. PMID: 17416441.

[25] MatlabBGL Library(http://www.stanford.edu/dgleich/programs/matlab bgl/).

[26] G. D. Bader, C.W. Hogue, An automated method for finding molecular complexes in large protein interaction networks, BMC Bioinformatics 4 (2).

[27] P. Thomas, M. J. Canpbell, A. Kejariwal, M. Huaiyu, B. Karlak, R. Daverman, K. Diemer, A. Muruganujan, N. A., Panther: a library of protein families and subfamilies indexed by function, Genome Res. 13 (2003) 2129–2141.

[28] Dempsey, K, Thapa, I, Bastola, D, and Ali, H. (2011) Identifying Modular Function via Edge Annotation in Gene Correlation Networks using Gene Ontology Search. 2011 BIBM Workshop on Data Mining for Biomarker Discovery: November 2011. Atlanta, GA

[29] A.Barabasi ,R.Alber ,"Emergence of scaling in random networks",1999

[30] K. Dempsey, K. Duraisamy, H. Ali, S. Bhowmick, A parallel graph sampling algorithm for analyzing gene correlation networks. International Conference in Computational Science 2011. ICCS'11. 2011.

[31] K. Duraisamy, K.Dempsey, H. Ali, S. Bhowmick, A noise reducing sampling approach for uncovering critical properties in large scale biological networks. The 2011 International Conference on High Performance Computing & Simulation. HPCS'11.

[32] K.Dempsey, K.Duraisamy, S.Bhowmick, H.Ali, The Developement of Parallel Adaptive Sampling Algorithms for Analyzing Biological Networks . The 2012 International Workshop on High Performance Computational Biology.HICOMB'12.

[33] Y. Saad, "Iterative Methods for Sparse Linear Systems", PWS Publishing Company, 1995